Fall 2019

# Exploration for alteration halos around the AG-W deposits in Southeastern Missouri, USA

Daniel Joseph Warbritton



Department:

# EXPLORATION FOR ALTERATION HALOS AROUND THE AG-W DEPOSITS IN SOUTHEASTERN MISSOURI, USA

by

DANIEL JOSEPH WARBRITTON

A THESIS

Presented to the Faculty of the Graduate School of the

MISSOURI UNIVERSITY OF SCIENCE AND TECHNOLOGY

In Partial Fulfillment of the Requirements for the Degree

MASTER OF SCIENCE IN GEOLOGY AND GEOPHYSICS

2019

Approved by:

Marek Locmelis, Advisor
Cheryl Seeger
John Hogan

# ABSTRACT

The St. Francois Mountains in SE Missouri are an extensive terrane of granitic ring complexes and associated rhyolites. They were an important source of Ag, W, and Sn and mined intermittently from the 1800s until the 1950s. The Ag-W ores occur in the Silvermine Granite and rhyolite roof rocks. The deposits are classified as a xenothermal ore system with mineralization occurring in quartz veins and surrounding greisen (up to 2.5 m). Exploration for hydrothermal ore deposits often focuses on the identification of alteration halos in the surrounding host rocks. In the vast majority of xenothermal ore deposits, such as in the Silver Mine District, the extent of alteration halos is often very small (cm to m scale) due to the rapid cooling experienced by the ore bearing fluids. As a consequence, such alteration halos are difficult to identify in the field.

This study investigates alteration halos around Silver Mine District Ag-W-Sn veins using petrographic observations and bulk rock chemistry. The goal is to develop an empirical, field-based exploration model than can provide a basis for identifying vectors towards ore zones. Samples were collected in incremental steps of 1 m, 3 m, 5 m, 10 m, 15 m, 25 m, 50 m, 100 m, and 200 m away from the Einstein vein. Field observations show distinct color changes within the rock, most notably at the 1 m, 5-15 m, 25-50 m and 100-200 m increments. Petrographically, the samples do not show significant changes. Bulk rock analysis of the samples show that Li, Be, Sr, Ba, Zr, Tl, Sn, and Sb contents vary as a function of distance from the ore, thus providing additional vectors towards mineralized zones. Results of this project show that a combination of field-observations, mineralogy and geochemical essays can be used to guide the exploration for xenothermal ore systems.

# ACKNOWLEDGEMENTS

The writer wishes to express his sincere appreciation to Dr. Marek Locmelis, of Missouri University of Science and Technology, for his guidance, coordination, and general supervision of this work.

The writer would also like to express gratitude to Dr. Cheryl Seeger, of the Missouri Department of Natural Resources, and Dr. John Hogan, of Missouri University of Science and Technology, for their help and guidance of this work as well.

# TABLE OF CONTENTS

Page

# LIST OF ILLUSTRATIONS

# LIST OF TABLES

# 1. INTRODUCTION

The Silver Mine District, located in southeastern Missouri, USA, is a well characterized natural laboratory that allows for development and testing of novel exploration tools for xenothermal ore systems. The term "xenothermal" was first coined by Buddington (1935) who discussed limitations of the then existing classification that limited ore-forming fluids to: (i) hypothermal – substantial depths (> 4500 m) and elevated temperatures (400°-600° C); (ii) mesothermal – intermediate depths (1500-4500 m) and temperatures (200°-400° C); (iii) epithermal – shallow depths (< 1500 m) and temperatures (50°-200° C). He proposed that a fourth group of hydrothermal ore deposits exists; i.e., deposits that were emplaced at relatively shallow depths (approximately ≤ 1500 m) and high temperatures (approximately 300°-500° C) and termed these *xenothermal* ore deposits. Buddington (1935) found evidence for these new types of deposits from the porous and fractured rocks found in both the outcrop and hand sample scale at the Au-W deposits of the Northern Black Hills quartz veins of the Bonanza District, Colorado, and the ferberite deposits of Boulder County, Colorado, which were found to be cause by hydrothermal activity within a high temperature and low pressure environment. Many of the minerals (e.g., magnetite, apatite, tourmaline, and topaz) that are usually considered to be found in high temperature deposits, were also found in the xenothermal deposits (Buddington, 1935). The main differences found within xenothermal deposits as opposed to typical hypothermal deposits are that these minerals are usually found to be well crystallized and medium- to coarse-grained (1-5 mm to > 5 mm) crystals in the former, and are commonly fine-grained (< 1 mm) and anhedral in the latter deposit type (Buddington, 1935).

Another common characteristic of xenothermal ore deposits is their telescoping nature (Guilbert and Park, 1986). Telescoping refers to minerals of one ore-zone overlapping those of another. The formation of the deposit is such that the shallowest part may be subjected to steep temperature/pressure gradients causing rapid deposition of ore minerals and a shortening of the ore zone; conversely, deeper in the deposit, temperature/pressure gradients are less steep and deposition occurs at a slower pace with well-defined separation of minerals and gradational zonal boundaries (Guilbert and Park, 1986).

Traditionally, exploration for hydrothermal ore deposits often focuses on the identification of alteration halos in the surrounding host rocks (White and Hedenqist, 1995; Large et al., 2001; Rowe and Zhou, 2007; Pour and Hashim, 2011). Alteration halos typically form around hydrothermal deposits in a zoned fashion, moving from high-grade alteration closest to the ore grading to low-grade away from the deposit. This zonation allows geologists to vector towards ore zones. The extent of alteration can range from meters away from the ore veins to several kilometers (Moon et al., 2006). However, in xenothermal ore deposits, such as in the Silver Mine District, extensive alteration halos are usually very small (cm to m) at the local scale and difficult to identify due to the rapid cooling of the ore bearing fluids during deposition. Although the Silver Mine District ore veins have been extensively studied in the past (Singewald and Milton, 1929; Lowell, 1976; Hagni, 1984; Kisvarsanyi and Hebrank, 1987; Shelton and Lofstrom, 1988), the nature and extent of the alteration halos at the local and regional scale around these Ag-W ore deposits remains to be established.

This thesis uses petrographical and geochemical observations in an attempt to define the extent, size, and characteristics of the alteration halos around the Ag-W ore deposits in the Silver Mine District. Due to the scarcity of exploratory practices utilized for these deposit types, this thesis will also provide an empirical study to use as a proxy for initial exploration of xenothermal ore deposits.

# 2. GEOLOGICAL BACKGROUND

## 2.1. REGIONAL GEOLOGY

The St. Francois Mountains in southeastern Missouri (Figure 2.1.) are an extensive terrane of granitic ring complexes and associated rhyolites that range in age from approximately 1.4 to 1.5 Ga (Kisvarsanyi, 1989; Rohs and Schmus, 2007; Bickford et al., 2015). Principal features of the terrane include fourteen central plutons, each 10-20 km in diameter, and a cluster of one complete and six partial ring intrusions, individually exceeding 20 km in diameter (Lowell, 1991). The volcanic rocks are predominately rhyolite ash-flow tuffs characterized by perthitic alkali feldspar phenocrysts and iron-rich mafic minerals (Kisvarsanyi, 1989). Kisvarsanyi (1989) classified the granitoids into three distinct types: (i) subvolcanic massifs, (ii) ring intrusions, and (iii) central plutons. The subvolcanic massifs are comagmatic with the rhyolites and are their intrusive equivalents; they are characterized by a granophyric texture and contain abundant perthitic alkali feldspar (Kisvarsanyi, 1989). The ring intrusions are intermediate- to high-silica rocks emplaced along ring fractures related to caldera collapse and cauldron subsidence; the granites are characterized as an amphibole-biotite granite (Kisvarsanyi, 1989). The so-called "*Silvermine Granite*", host rock for the Ag-W ore deposits investigated in this study, is classified as a ring intrusion (Kisvarsanyi, 1989; Lowell and Young, 1999). The central plutons are inferred to have been emplaced in resurgent cauldrons; they are characterized mainly as two-mica granites (Kisvarsanyi, 1989). The Precambrian rocks of the St. Francois Mountains within the Silver Mine District are overlain in areas by the Upper Cambrian Lamotte Sandstone, conglomerate, and by small patches of Tertiary Lafayette Gravel (Howe and Koenig, 1995).

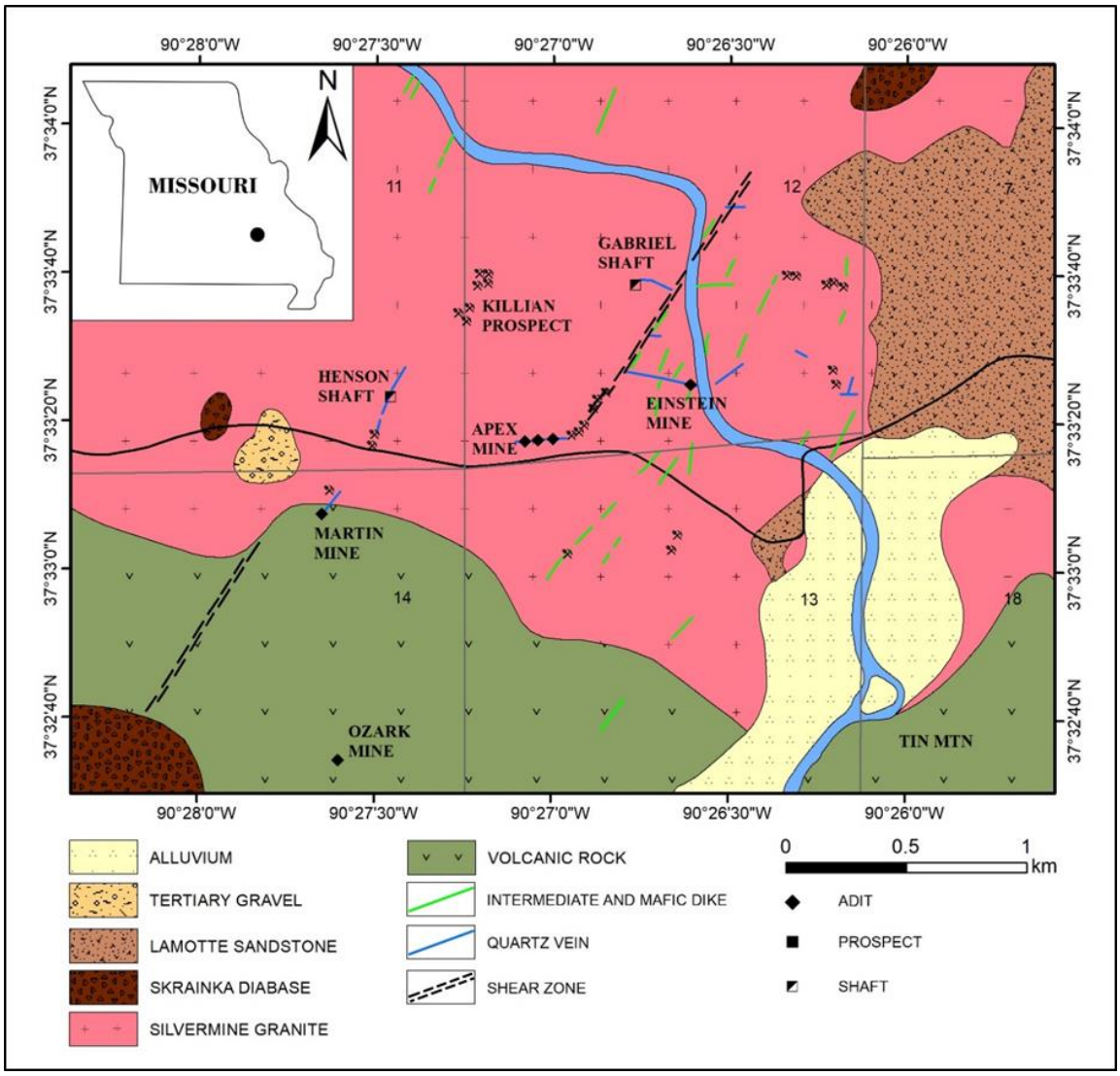


Figure 2.1. Geologic map of the Silver Mine District. Note: Locations of the abandoned Ag-W mines. Modified from Kisvarsanyi and Hebrank (1987).

## 2.2. THE SILVER MINE DISTRICT

Rocks exposed in this area consist mainly of the Precambrian Silvermine Granite and rhyolites that are intruded by diabase dikes, and Ag-W ore veins that are primarily composed of a greenish-gray greisen and milky-white quartz veins which crosscut the former and latter rocks (Hagni, 1984; Rohs, 2013; Figures 2.1., 2.2.). The Silvermine

Granite is a medium- to coarse-grained (i.e., 1-5 mm and ≥5 mm) rock varying in color from gray to grayish pink in outcrops and/or hand specimens (Figures 2.2., 2.3.). Mineralogically, the Silvermine Granite has been described as an amphibole-biotite granite with an average composition of 40% orthoclase-microperthite, 30% sodic oligolcase, 20% quartz, and 10% mafic minerals (Balogh et al., 1988). The age of the granite is approximately 1.5 Ga based on U-Pb zircon analysis (Bickford and Mose, 1975; Bickford, 1976). Most of the Ag-W ore veins were emplaced into the Silvermine Granite; however, several other veins also have been reported from the Marlow Mountains Rhyolite, which is located to the west of the study area (Hagni, 1984). The Marlow Mountain Rhyolite is described as a purple colored rhyolite porphyry containing a few small quartz phenocrysts (Balogh et al., 1988).

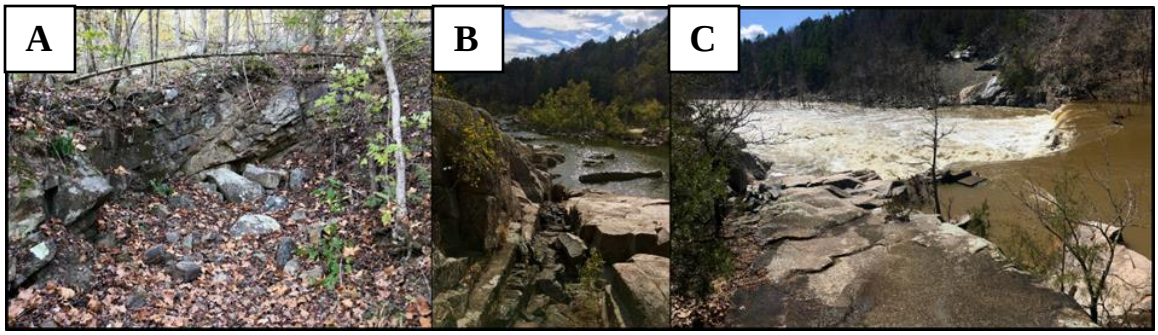

Figure 2.2. Cross-cutting relationships observed in the study area. (A) Greisen at the New Discovery Shaft entrance; to the left of the photo is the granite that was intruded by the ore-forming fluids. (B) Diabase dike that intruded the Silvermine Granite. (C) Taken on top of the Silvermine Granite with the diabase dike to the left and the ore vein to the top right.

**2.2.1. Mining History.** Mining in the Silver Mine District began in 1877. During this time, an estimated 3000 ounces of silver and 50 tons of lead were produced (Tolman,

1933). In 1894, the second wave of mining produced an estimated 120 short tons of tungsten concentrates (Kisvarsanyi, 1989). During World War I and World War II, the mines reopened in 1916 and 1941. Tungsten ore was mined during these times in order to assist with steel production for the war efforts (Shelton et al., 1988). Mining finally ceased in the area around 1957, and at the present time, the mines are not in operation and the shafts are inaccessible.

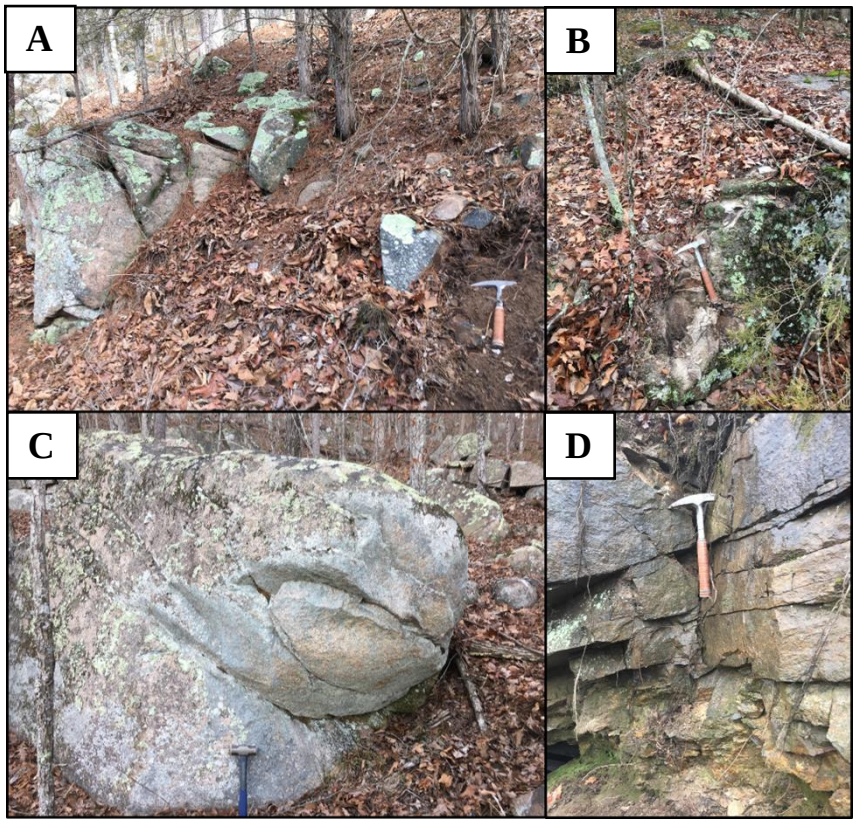


Figure 2.3. Respective examples of sampling sites for this study. Note: Outcrops and lack thereof, and general difficulty of terrain.

**2.2.2. Ag-W Ore in the Silver Mine District.** The ore of the xenothermal Ag-W deposits in the Silver Mine District occur as pods, lenses, and irregularly shaped bodies

within quartz veins (Shelton and Lofstrom, 1988). The deposits have been shown to have formed in a paragenetic sequence characterized by four stages: (1) greisen stage, (2) early vein stage, (3) main sulfide deposition stage, and (4) late quartz stage (Hagni, 1984; Figure 2.4.). The mineralization has been suggested to have formed at a depth of ca. 1250 m based on the fluid inclusions in sphalerite and fluorite that formed within the main sulfide deposition stage (Shelton and Lofstrom, 1988). The age of mineralization was determined by radiometric dating of zinnwaldite [$KLiFe^{2+}Al_2Si_3O_{10}F_{1.5}(OH)_{0.5}$] found within the ore yielding a K/Ar age of 1405±42 Ma and a Rb/Sr age of 1430±43 Ma (Tilton et al., 1962; Lowell and Gasparrini, 1982).

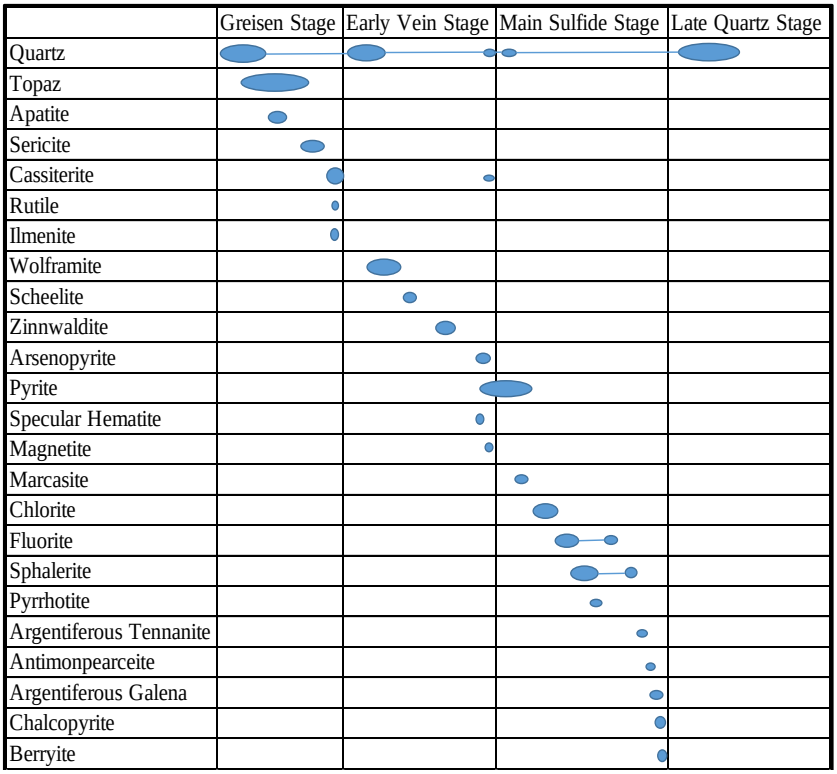


Figure 2.4. Paragenetic sequence of minerals deposited in the Ag-W deposits. Silver Mine District. Modified from Hagni (1984).

**2.2.2.1. Greisen stage.** The earliest stage of mineralization, the greisen stage, consisted of granite being intensively altered to a greenish-gray and medium-gray, topaz-quartz-sericite greisen (Hagni, 1982). Greisen that formed within the rhyolite, which is not a part of this study, are banded and composed of fine-grained topaz and quartz (Hagni, 1984). Minerals deposited during this stage include quartz, topaz, apatite, sericite, cassiterite, and ilmenite: (i) rutile and ilmenite occur as inclusions within cassiterite that are usually 1-4 µm across; (ii) topaz occurs as 20-65 µm grains where it replaces silicate phenocrysts and aphanitic groundmass of the rhyolite and 100-200 µm grains where silicate minerals, i.e. quartz, plagioclase, k-spar, are replaced; (iii) quartz is coarse-grained (Hagni, 1984). The fluid inclusion study completed by Lofstrom (1987) indicates that ore fluids were approximately $\geq 380°$ C during formation of the greisen.

**2.2.2.2. Early vein stage.** The early vein stage consisted of the deposition of quartz, wolframite, scheelite, zinnwaldite, arsenopyrite, specular hematite, magnetite, and pyrite (Hagni, 1984). Wolframite occurs as coarse prismatic crystals disseminated and clustered in quartz; zinnwaldite is deposited on wolframite prior to the deposition of minerals belonging to the subsequent main sulfide stage; specular hematite occurs in the earliest pyrite as atolls of plates with some of the hematite crystals having been partially to completely reduced to form specular magnetite pseudomorphs (Hagni, 1984). Fluid emplacement temperatures during this stage occurred between 380° C to 250° C (Lofstrom, 1987).

**2.2.2.3. Main sulfide deposition stage.** The main sulfide stage is characterized by early deposition of pyrite, marcasite, chlorite, fluorite, sphalerite, and pyrrhotite followed by the silver-bearing minerals argentiferous tennantite, antimonpearcite, argentiferous

chalcopyrite, argentiferous galena, and a Ag-Cu-Bi sulfide (Hagni, 1984). During the later stages of this phase, the coarse-grained pyrite is partially replaced by the silver-bearing minerals; initial replacements typically form irregularly shaped patches within the pyrite with local vein textures proving this replacement process; rare tiny vugs within the pyrite contain the simple superposition sequence of sphalerite, galena, and chalcopyrite (Hagni, 1984). Base-metal and silver-bearing minerals were deposited at ore-fluid temperatures between 270° C to 150° C (Shelton and Lofstrom, 1988).

**2.2.2.4. Late quartz stage.** The late quartz stage is characterized by deposition of quartz (Hagni, 1984). In an oxygen isotope study, Shelton and Lofstrom, (1988), suggested that a noticeable decrease of $\delta^{18}O_{water}$ values during the end of the main sulfide deposition stage and late quartz stage indicate a progressive increase of meteoric water interaction within the ore depositional system. This increase of meteoric water and magmatic water interaction was a likely contributing factor to the cooling of the hydrothermal system and end of ore deposition (Shelton and Lofstrom, 1988).

# 3. METHODS

## 3.1. FIELD WORK

The Einstein Vein and surrounding Silvermine Granite host rock were investigated during this study (Figure 3.1.) using previous reports and maps as guides (i.e., Singewald and Milton, 1929; Shelton and Lofstrom, 1988; Balogh et al., 1988). Sampling began at the portion of the Einstein Vein found at the New Discovery Shaft and at the continuation of the Einstein Vein on the east side of the St. Francois River. Samples were collected at the surface as there is no access to the mine shafts within the Silver Mine Recreation Area.

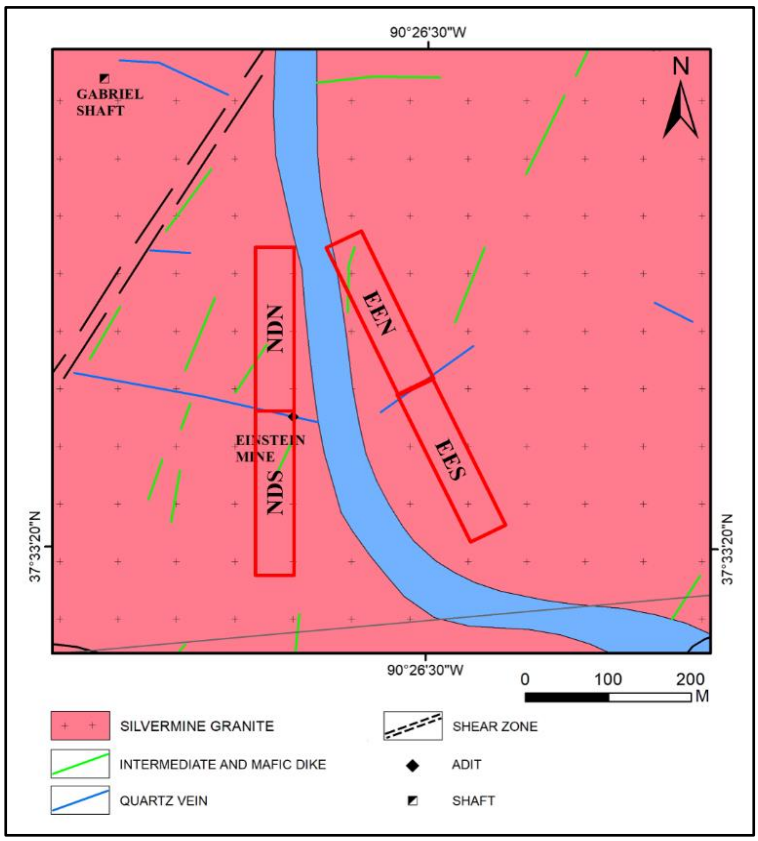


Figure 3.1. Geologic map of the study area. Modified from Kisvarsanyi and Hebrank, (1987). Note: Red boxes indicate sampling area for the respective sample suites.

### 3.2. SAMPLING

Samples were collected from outcrops at the north and south portions of the N60E striking greisen vein moving perpendicularly in incremental steps of 1 m, 3 m, 5 m, 10 m, 15 m, 25 m, 50 m, 100 m, and 200 m away from the vein (Figure 3.1.; Table 3.1.). Therefore, the sample suites are named New Discovery South, New Discovery North, Einstein East South, and Einstein East North. Rock samples averaging ~6 x 8 cm were taken at each meter mark. Only outcropping rocks with no signs of significant weathering were selected for this study. Sample locations and characteristics are summarized in Table 3.1.; pictures of samples can be found in Figure 4.1.

### 3.3. MICROSCOPY

All rock samples were prepared as polished thin sections and studied using a Leica DMV-6 microscope in the Ore Microscopy Laboratory in the Department of Geosciences and Geological and Petroleum Engineering at Missouri University of Science and Technology.

### 3.4. BULK ROCK ANALYSIS

The major, minor, and trace element chemistry of all samples was determined at Geoscience Laboratories (Geolabs), Sudbury, Canada. Major element compositions were determined by X-Ray Fluorescence; minor and trace element compositions were determined by inductively coupled plasma-mass spectrometry (ICP-MS) with closed vessel multi-acid digestion; gold and silver concentrations were ascertained utilizing gravimetric fire assay.

Table 3.1. Location and petrography of the sample greisens and granites. Note: GPS accuracy is within 10 m.

| Sample | GPS | Lithology | Mineral Assemblages |
|---|---|---|---|
| | | | |
| **New Discovery South** | | | |
| **NDS0** | 37°33'26.79"N 90°26'36.11"W | Greisen | Qtz-Tpz ± Ser-Fl-Sph-Mus-Zr |
| **NDS1** | 37°33'26.50"N 90°26'35.96"W | Granite | Qtz-Plag-Bt ± Tpz-Ser-Sph |
| **NDS2** | 37°33'26.87"N 90°26'36.54"W | Granite | Qtz-Plag-Bt-Hbl ± Ser-Chl-Ep-Zr |
| **NDS3** | 37°33'26.54"N 90°26'36.56"W | Granite | Qtz-Plag-Bt-Hbl ± Ser-Chl-Ep-Zr |
| **NDS4** | 37°33'26.45"N 90°26'35.93"W | Granite | Qtz-Plag-Bt-Mic-Hbl ± Ser-Chl-Ep-Mus |
| **NDS5** | 37°33'26.37"N 90°36'36.28"W | Granite | Qtz-Plag-Bt-Mic-Hbl ± Chl-Ep-Mus-Cal |
| **NDS6** | 37°33'25.67"N 90°26'36.06"W | Granite | Qtz-Plag-Bt-Mic-Hbl ± Chl-Ep-Zr |
| **NDS7** | 37°33'24.91"N 90°26'36.30"W | Granite | Qtz-Plag-Bt-Mic-Hbl ± Chl-Ep-Zr |
| **NDS8** | 37°33'23.45"N 90°26'35.76"W | Granite | Qtz-Plag-Bt-Mic-Hbl ± Chl-Ep-Zr |
| **NDS9** | 37°33'20.26"N 90°26'33.27"W | Granite | Qtz-Plag-Bt-Mic-Hbl ± Chl-Ep-Zr |
| | | | |
| **New Discovery North** | | | |
| **NDN0** | 37°33'26.81"N 90°26'36.09"W | Griesen | Qtz-Tpz ± Ser-Fl-Sph-Mus-Zr |
| **NDN1** | 37°33'26.92"N 90°26'36.00"W | Granite | Qtz-Plag-Bt-Mic ± Tpz-Ser-Sph |
| **NDN2** | 37°33'27.19"N 90°26'35.81"W | Granite | Qtz-Plag-Bt-Mic-Hbl ± Ser-Zr |
| **NDN3** | 37°33'26.70"N 90°26'36.45"W | Granite | Qtz-Plag-Bt-Mic-Hbl ± Ser-Zr |
| **NDN4** | 37°33'27.21"N 90°26'36.17"W | Granite | Qtz-Plag-Bt-Mic-Hbl ± Ser-Zr |
| **NDN5** | 37°33'27.66"N 90°26'35.91"W | Granite | Qtz-Plag-Bt-Mic ± Ser-Chl-Zr |
| **NDN6** | 37°33'28.08"N 90°26'36.11"W | Granite | Qtz-Plag-Bt-Mic-Hbl ± Ser-Chl-Zr |
| **NDN7** | 37°33'28.69"N 90°26'35.84"W | Granite | Qtz-Plag-Bt-Mic ± Ser-Chl |
| **NDN8** | 37°33'29.64"N 90°26'35.58"W | Granite | Qtz-Plag-Bt-Mic ± Ser-Chl |
| **NDN9** | 37°33'31.17"N 90°26'35.67"W | Granite | Qtz-Plag-Bt-Mic ± Ser-Chl |

Qtz, quartz; Tpz, topaz; Plag, plagioclase; Bt, biotite; Ser, sericite; Hbl, hornblende; Mic, microcline; Fl, fluorite; Sph, sphalerite; Mus, muscovite; Chl, chlorite; Ep, epidote; Cal, calcite; Zr, zircon.

Table 3.1. Location and petrography of the sample greisens and granites. Note: GPS accuracy is within 10 m. (cont.).

| Sample | GPS | Lithology | Mineral Assemblages |
|---|---|---|---|
| | | | |
| **Einstein East South** | | | |
| **EES0** | 37°33'26.13"N 90°26'29.95"W | Greisen | Qtz-Tpz ± Ser-Fl-Sph-Mus-Zr |
| **EES1** | 37°33'25.67"N 90°26'30.47"W | Granite | Qtz-Plag-Bt ± Tpz-Ser-Sph |
| **EES2** | 37°33'25.47"N 90°26'30.43"W | Granite | Qtz-Plag-Bt-Hbl ± Ser-Chl-Ep-Zr |
| **EES3** | 37°33'25.16"N 90°26'29.97"W | Granite | Qtz-Plag-Bt-Mic-Hbl ± Ser-Zr |
| **EES4** | 37°33'25.17"N 90°26'29.77"W | Granite | Qtz-Plag-Bt-Mic-Hbl ± Ser-Zr |
| **EES5** | 37°33'25.07"N 90°26'29.42"W | Granite | Qtz-Plag-Bt-Mic ± Ser-Chl-Zr |
| **EES6** | 37°33'24.53"N 90°26'29.59"W | Granite | Qtz-Plag-Bt-Mic-Hbl ± Ser-Chl-Zr |
| **EES7** | 37°33'24.08"N 90°26'28.82"W | Granite | Qtz-Plag-Bt-Mic ± Ser-Chl |
| **EES8** | 37°33'21.95"N 90°26'27.93"W | Granite | Qtz-Plag-Bt-Mic ± Ser-Chl |
| **EES9** | 37°33'20.14"N 90°26'21.17"W | Granite | Qtz-Plag-Bt-Mic ± Ser-Chl |
| | | | |
| **Einstein East North** | | | |
| **EEN0** | 37°33'25.98"N 90°26'31.56"W | Greisen | Qtz-Tpz ± Ser-Fl-Sph-Mus-Zr |
| **EEN1** | 37°33'26.73"N 90°26'30.96"W | Granite | Qtz-Plag-Bt ± Tpz-Ser-Sph |
| **EEN2** | 37°33'26.80"N 90°26'31.26"W | Granite | Qtz-Plag-Bt-Mic-Hbl ± Ser-Zr |
| **EEN3** | 37°33'27.13"N 90°26'30.70"W | Granite | Qtz-Plag-Bt-Mic-Hbl ± Ser-Zr |
| **EEN4** | 37°33'26.97"N 90°26'31.43"W | Granite | Qtz-Plag-Bt-Mic-Hbl ± Ser-Chl-Ep-Mus |
| **EEN5** | 37°33'27.33"N 90°26'30.87"W | Granite | Qtz-Plag-Bt-Mic ± Ser-Chl-Zr |
| **EEN6** | 37°33'28.14"N 90°26'31.06"W | Granite | Qtz-Plag-Bt-Mic-Hbl ± Ser-Chl-Zr |
| **EEN7** | 37°33'28.71"N 90°26'31.10"W | Granite | Qtz-Plag-Bt-Mic-Hbl ± Chl-Ep-Zr |
| **EEN8** | 37°33'30.71"N 90°26'32.12"W | Granite | Qtz-Plag-Bt-Mic ± Ser-Chl |
| **EEN9** | 37°33'32.61"N 90°26'32.32"W | Granite | Qtz-Plag-Bt-Mic ± Ser-Chl |

Qtz, quartz; Tpz, topaz; Plag, plagioclase; Bt, biotite; Ser, sericite; Hbl, hornblende; Mic, microcline; Fl, fluorite; Sph, sphalerite; Mus, muscovite; Chl, chlorite; Ep, epidote; Cal, calcite; Zr, zircon.

# 4. RESULTS

## 4.1. PETROGRAPHIC OBSERVATIONS

Petrographically, samples gathered from the ore zone up to 200 m away show only minor variation, outside of the closest samples up to 3 m away (Table 3.1.; Figures 4.1., 4.2.). The most noticeable changes approaching the ore zone are the color changes within the host rock; color variation can be used as an indicator of alteration zone as shown in Figure 4.1.

**4.1.1. The Ore Bearing Rock.** (NDS0, NDN0, EES0, EEN0; Figure 4.1., 4.2.) is a black to light-gray greisen consisting mainly of quartz and topaz, minor sphalerite (within this hand sample), fluorite, and sericite, and trace muscovite and zircons. The topaz and quartz occur as both groundmass and fine- to coarse-grained anhedral to subhedral crystals. The minor fluorite fills interstitial spaces between crystals and is fine-grained and anhedral. Sphalerite and micas are fine- to medium-grained with anhedral to subhedral crystals. Zircon rarely occurs within the greisen as fine-grained, subhedral to euhedral crystals.

**4.1.2. Adjacent to the Ore Zone.** (NDS1, NDN1, EES1, EEN1; Figure 4.1., 4.2.) the granite is a moderate yellow to pale greenish yellow colored rock that consists of quartz, plagioclase, topaz, biotite, sericite, and sphalerite. Quartz is fine- to coarse-grained and subhedral. Plagioclase occurs as fine- to coarse-grained anhedral to euhedral crystals. Biotite is anhedral to euhedral with fine- to medium-grained crystals. Topaz occurs mainly as interstitial groundmass with trace medium- to coarse-grained, anhedral

to subhedral crystals. Sericite and sphalerite are anhedral and fine-grained crystals within this sample.

**4.1.3. Three to Ten Meters Away from the Greisen.** (Figure 4.1., 4.2.), the granite ranges from a grayish yellow to a pale yellowish brown. The mineralogy of these samples is generally dominated by quartz, plagioclase, microcline, biotite, chlorite, epidote, hornblende, clinopyroxene, sericite, zircon, muscovite, and iron oxides. Quartz, plagioclase, and microcline occur as fine- to coarse-grained, subhedral to euhedral crystals; much of the plagioclase and microcline have been seritized. Biotite and minor muscovite occur as fine- to medium-grained subhedral crystals. Epidote and chlorite in many places are replacement minerals of relict biotite crystals. Minor hornblende is fine- to medium-grained with anhedral to subhedral crystals. Minor clinopyroxene and zircon both occur as fine-grained anhedral to subhedral crystals.

**4.1.4. From 15 m to 50 m Away from the Ore Zone.** (Figure 4.1., 4.2.), the granite varies from a pale red to moderate red. The mineralogy is dominated by quartz, plagioclase, and microcline with minor biotite, epidote, chlorite, hornblende, and muscovite, and trace calcite and zircon. Quartz forms fine- to medium-grained anhedral to euhedral crystals. Plagioclase and microcline are medium- to coarse-grained, subhedral to euhedral crystals that, in roughly 25% of the crystals, show replacement through saussuritization and seritization. Biotite occurs as fine- to medium-grained crystals that are subhedral to euhedral; locally, biotite has been replaced by chlorite. Hornblende is medium- to coarse-grained and is subhedral. Muscovite, calcite, and zircon are fine-grained and subhedral to euhedral.

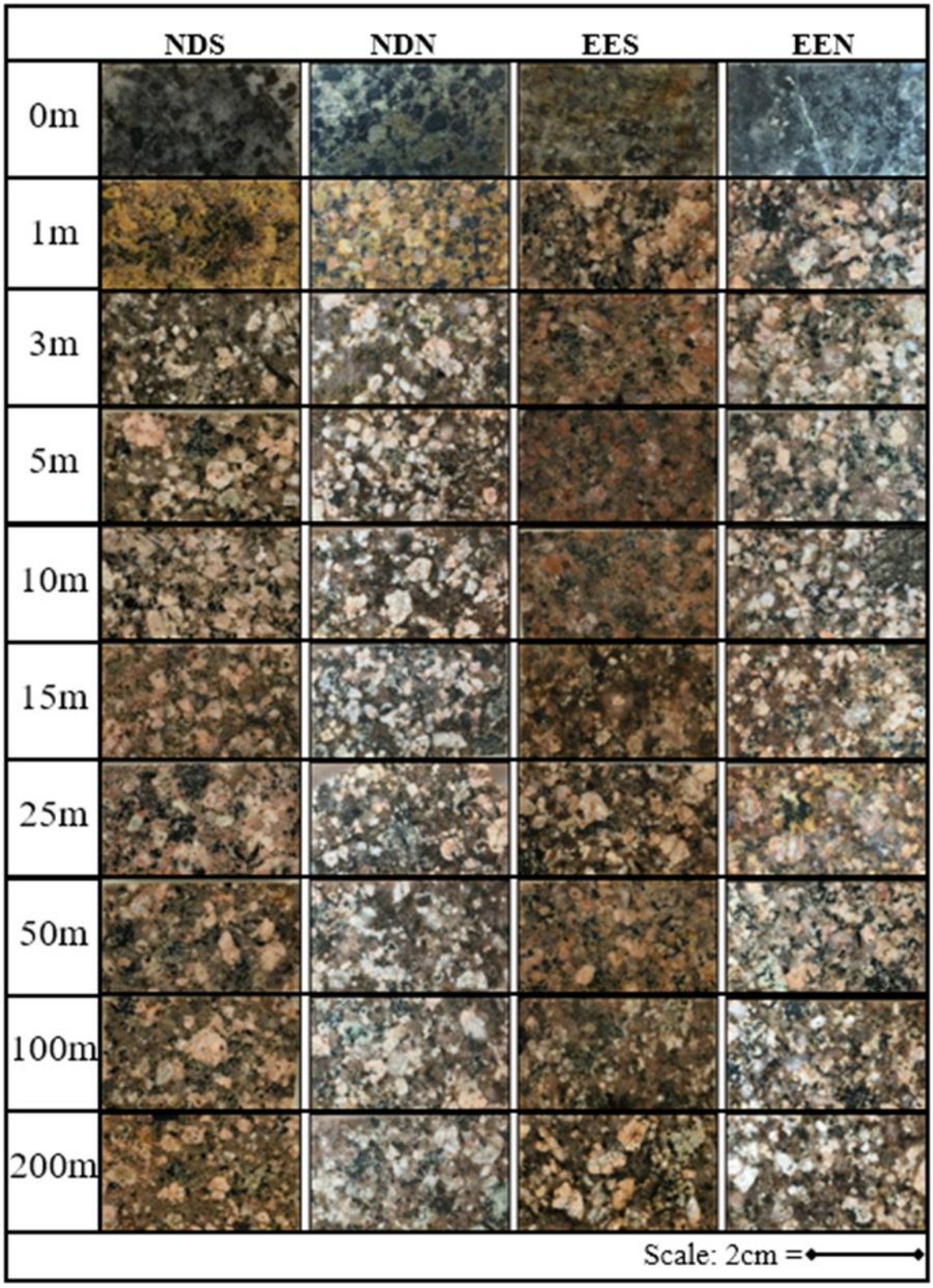


Figure 4.1. Hand sample pictures of the 40 samples gathered for this study. NDS0, NDN0, EES0, and EEN0 are in the ore zone; the rest of the samples are host rock.

**4.1.5. At 100 m and 200 m Distance from the Ore.** (NDS8, NDN8, EES8, EEN8, and NDS9, NDN9, EES9, EEN9; Figure 4.1., 4.2.), the Silvermine Granite is a grayish pink color consisting of quartz, plagioclase, microcline, biotite, epidote, chlorite, hornblende, and zircon. The plagioclase and microcline are fine- to coarse-grained crystals that are subhedral to euhedral. Quartz is fine-grained and subhedral to euhedral. The minor biotite is fine- to medium-grained that is subhedral to euhedral; some of the biotite has been chloritized. Epidote occurs as a minor replacement product of plagioclase. Hornblende is medium-grained with anhedral to subhedral crystals. Trace zircon occurs as fine-grained crystals that are subhedral to euhedral.

## 4.2. BULK ROCK GEOCHEMICAL DATA

Geochemically, the Silvermine Granite (excluding ore veins) plots as a typical granite on the Total Alkali Silica (TAS) diagram from Middlemost (1994); greisen from the ore veins plots within the granodiorite zone of the diagram. Select trace elements have been identified that show enrichment or depletion when moving towards the ore zone. There is little variation seen within the rare earth element (REE) diagrams with all sample suites.

**4.2.1. Major/Minor Element Chemistry.** When comparing the $Na_2O + K_2O$ contents vs. $SiO_2$ of the rocks (Figure 4.3.), all of the samples from 1 m to 200 m plot within the granite portion of the diagram. The four outliers from the main group are from each of the greisen samples from their respective suites; these plot within the granodiorite portion of the diagram.

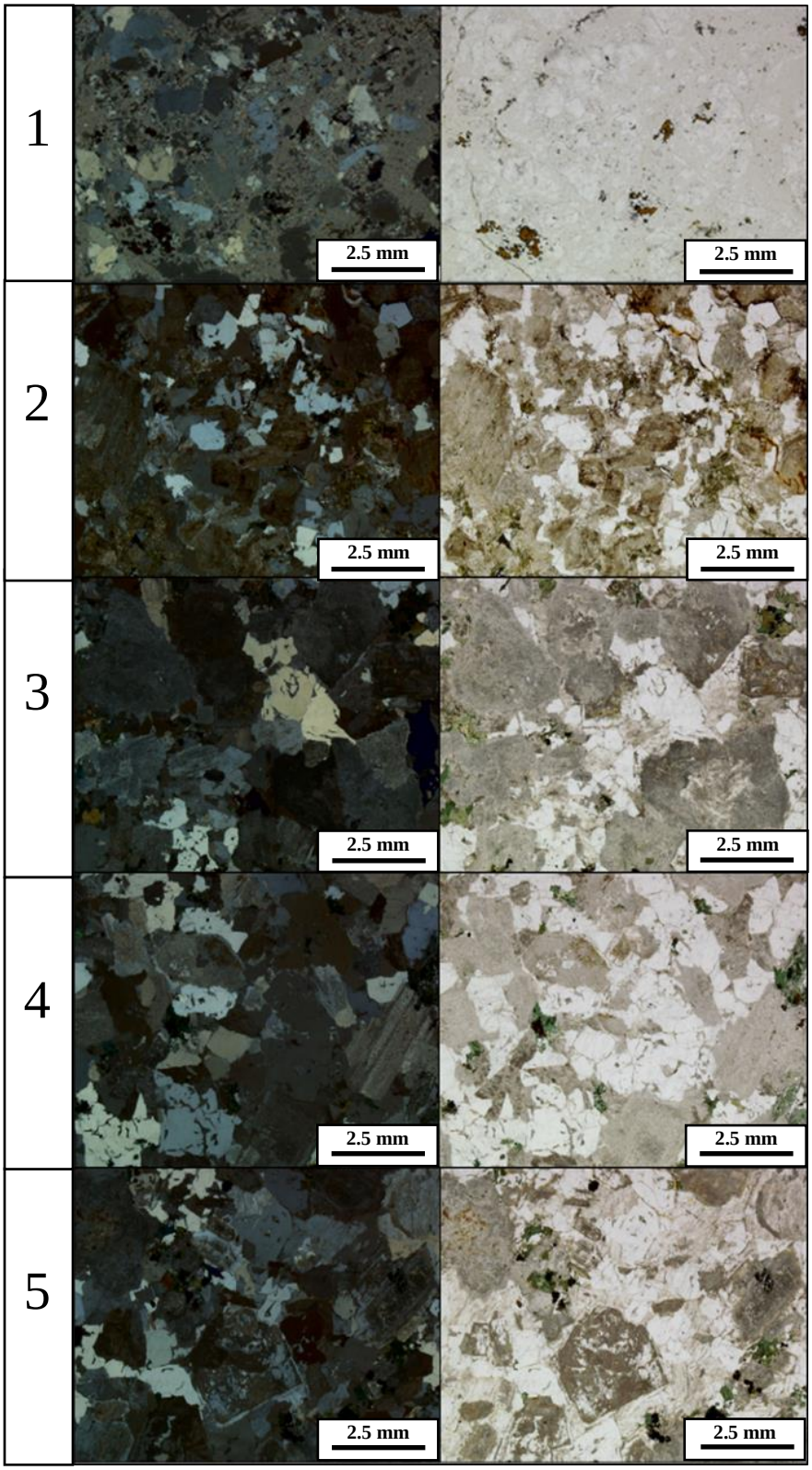


Figure 4.2. Representative thin sections. Detail the petrology of ore and host rocks within the study area. 1) Ore vein; 2) 1 m away; 3) 5-15 m away; 4) 25-50 m; 5) 100-200 m away.

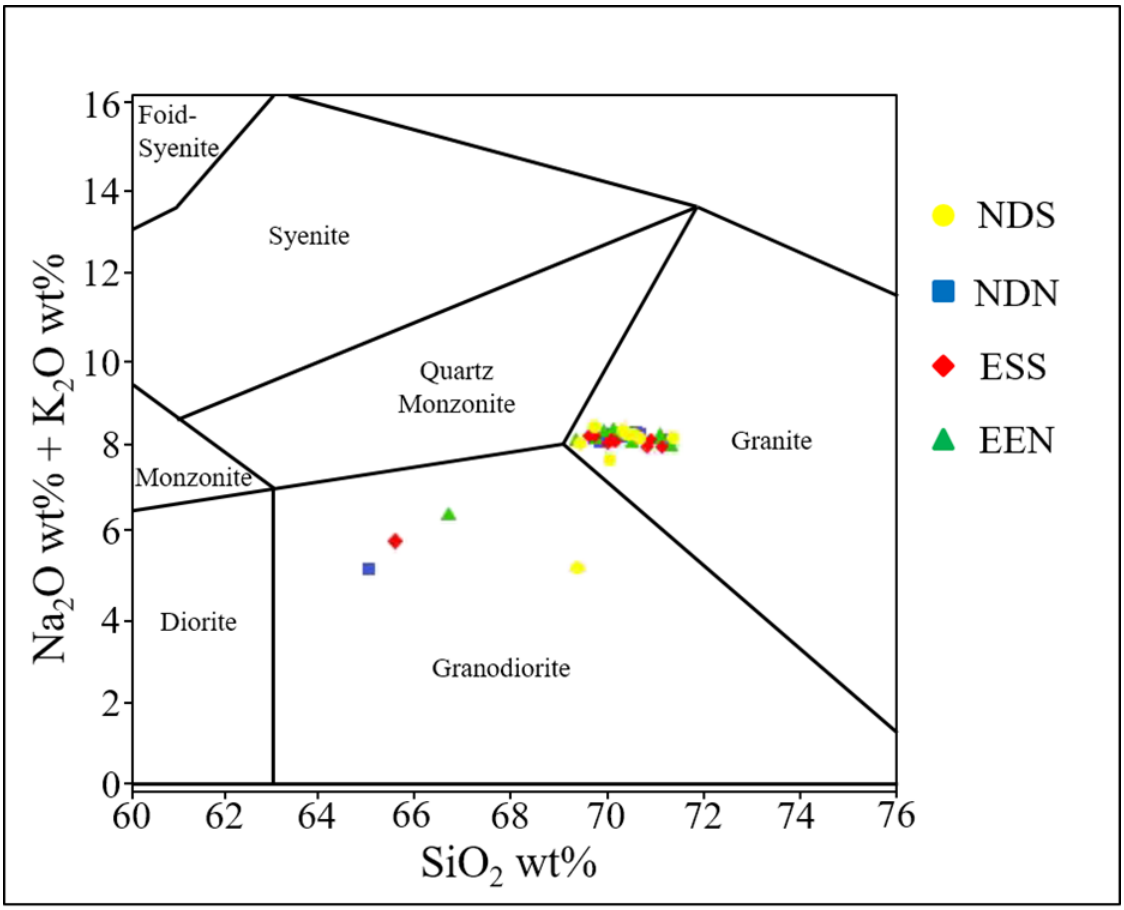


Figure 4.3. Plutonic Total Alkali Silica (TAS) diagram. From Middlemost, (1994) showing major element concentrations of the Silvermine samples of this study. Note: Grouping of 1 m-200 m samples within the granite area; four outliers from the greisen lie within the granodiorite area.

**4.2.2. Trace Element Chemistry.** The samples investigated in this study show overall similar trace element patterns when normalized against the composition of the upper crust (Taylor and McLennan, 1985; Figure 4.4.). The overall behavior of the trace element diagram is relatively flat with a few notable anomalies: a strong positive anomaly with Rb; relatively strong negative anomalies with Nb, Sr, and P. Within the ore zone rocks of each sample suite, there is a noticeable enrichment of barium and potassium. Noticeable negative anomalies exist for Nb, Sr, and P, whereas Sm, Tb, Y, and Yb display positive anomalies.

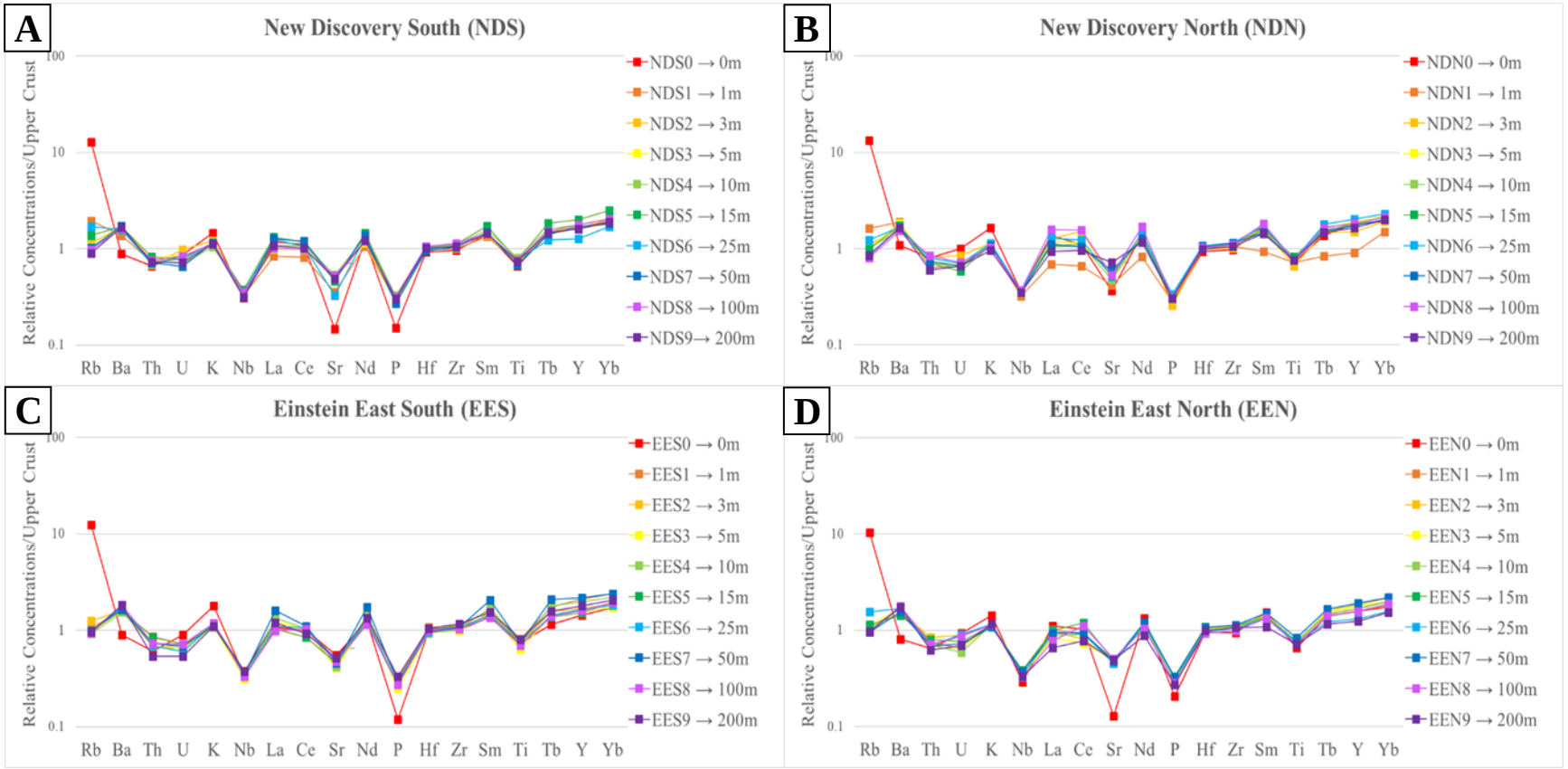


Figure 4.4. Concentrations of trace elements relative to the composition of the upper crust. From Taylor and McLennan (1985). Sample NDS0, NDN0, EES0, EEN0 are location in the ore zone; remaining samples are host rocks.

Figure 4.5. shows the mobility of pathfinder trace elements (i.e., trace elements used in exploration for certain ore deposit types) in relation to the ore zone and proximity. Trace elements that show a marked enrichment when moving towards the ore zone include: lithium, beryllium, thallium, tin, and antimony. Those that show a marked depletion moving towards the ore zone include strontium and barium. Zirconium shows a minor depletion towards the ore zone.

**4.2.3. Rare Earth Elements.** The rare earth elements (REE) diagrams normalized to the composition of the C-1 chondrite (McDonough and Sun, 1995) are overall similar for all sample suites (Figure 4.6). All samples are characterized by a moderate dip from La to Gd, and a flat trend from Gd to Lu with a negative anomaly at Eu and a positive anomaly at Th. Some samples display minor negative or positive Ce anomalies.

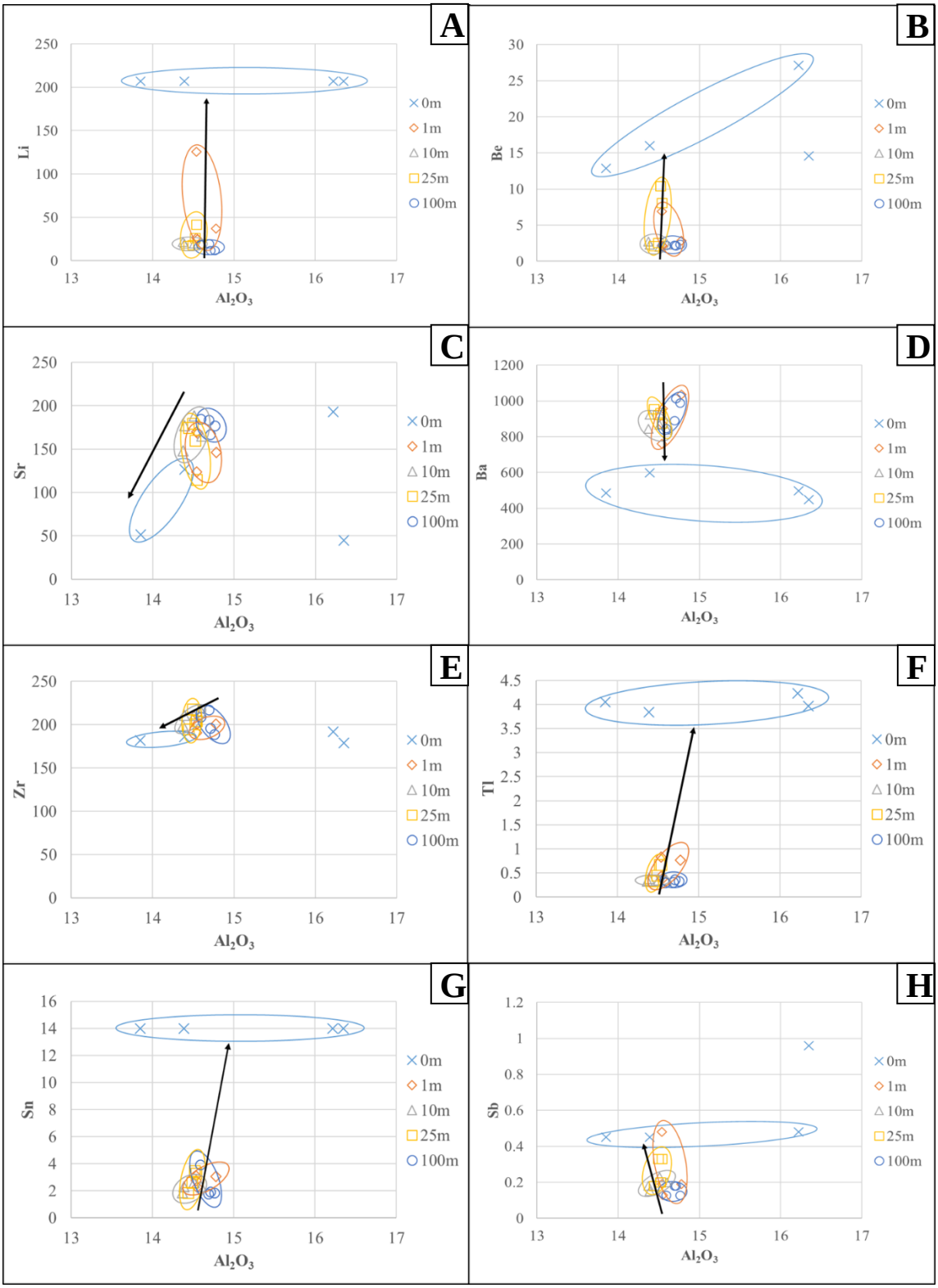


Figure 4.5. Binary plots of elements within the Silvermine ore system. Plotted against the immobile Al. Note: Black arrows denote enrichment or depletion moving towards the ore; Blue circles = grouping of ore zone samples (0 m); Orange circles = grouping of 1 m samples; Gray circles = grouping of 10 m samples; Yellow circles = grouping of 25 m samples; Dark blue circles = grouping of 100 m samples.

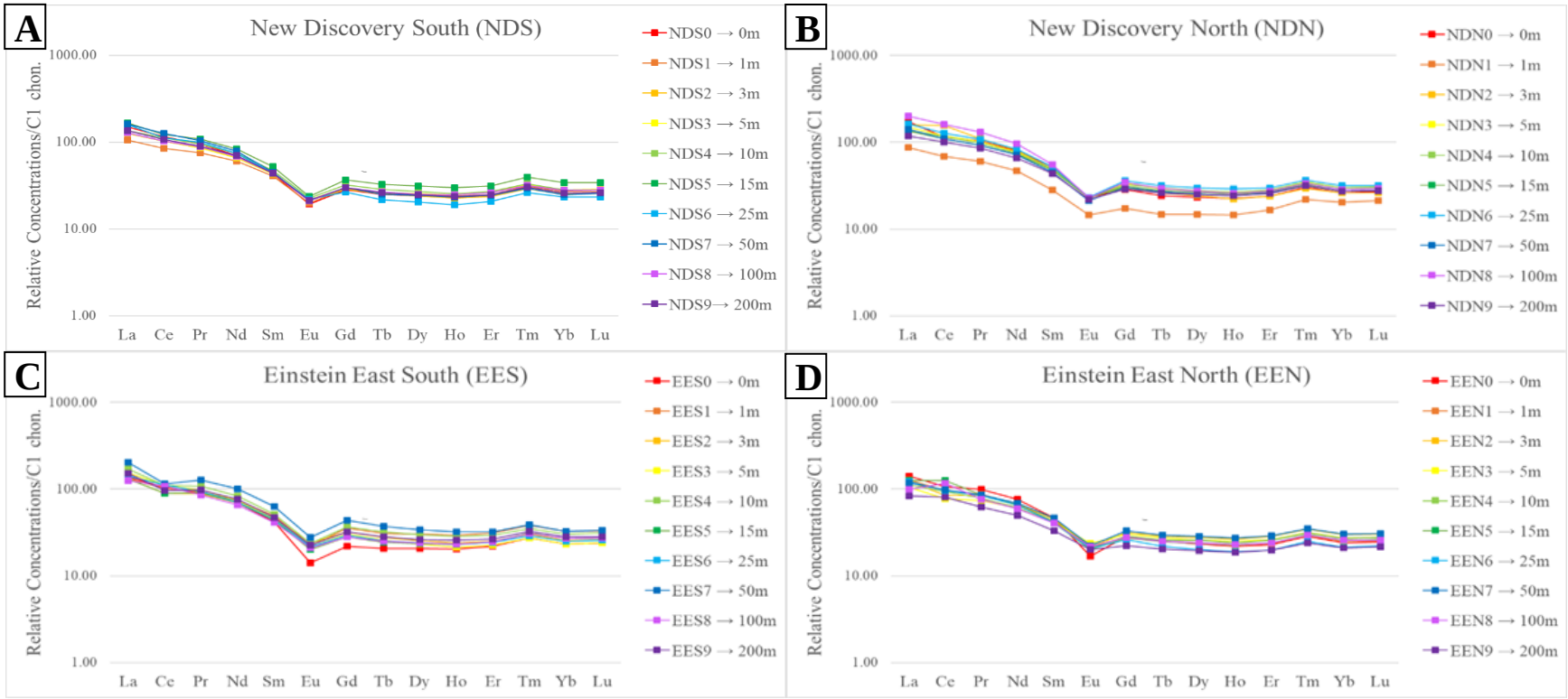


Figure 4.6. Rare earth element diagrams. Show bulk rock concentrations of REEs relative to C1 chondrite of McDonough and Sun (1995). Sample NDS0, NDN0, EES0, and EEN0 are located in the ore zone; remaining samples are host rock.

# 5. DISCUSSION

Defining the alteration halos around a xenothermal deposit is an important aspect of exploration geology. However, such alteration halos are not always well-defined or may cover large areas and therefore may be easily hidden under cover and missed. This is due to the rapid-cooling nature of the ore fluids and surrounding country rock because of the relatively shallow emplacement depth; because of this, the ore veins and halos are often small and easy to miss.

## 5.1. FIELD AND MINERALOGIC OBSERVATIONS

In order to define the alteration halos around the Ag-W ore deposits within the Silver Mine District, observations were made at the macro-scale and at the micro-scale. The most notable change seen in outcrop and hand sample is the change in color of the Silvermine Granite moving towards the ore veins. The change in color is interpreted to reflect that, close to the ore, the granite was modified by the high temperature ($\geq 400°C$) during the ore forming event that caused the alteration of minerals within the host rock. It is noted that in the field, there are no real clear indicators of mineralogic changes as commonly observed in porphyry deposits (i.e., propylitic zone, phyllic zone, etc.; Robb, 2013). Mineralogically, the Silvermine Granite shows slight variation until the ore zone is reached. Around 25 m before the ore zone, the typically grayish pink granite changes color to a red. At about 5 m away from the ore zone, the granite changes to a yellowish color. Within the ore zone, the granite is intensely altered to a grayish olive greisen.

## 5.2. GEOCHEMICAL OBSERVATIONS

Most Silvermine Granite samples plot as granite in the TAS diagram shown in Figure 4.3. The four samples taken from the ore vein plot in the granodiorite field. Several elements show promise as geochemical vectors towards mineralized veins, including Rb, Ba, Li, Be, Sr, Zr, Tl, Sn, and Sb. Li, Be, Tl, Sn, and Sb all show depletion moving towards the ore zone, whereas Sr, Ba, and Zr show enrichment when moving towards the ore zone.

## 5.3. IMPLICATIONS FOR EXPLORATION

The identification of reliable lithogeochemical exploration tools for polymetallic xenothermal ore deposits is a long-standing goal of economic geology. This project highlights that both field observations and geochemical patterns can be used due to the systematic and relatively uniform patterns seen in all four sampling profile gathered within the Silver District. Therefore, we suggest that integration of geochemical and field observations can be used by exploration geologists in search of similar xenothermal ore deposits. To fully understand the usefulness of this study in exploration, follow up studies should conduct a thorough meter-scaled surface sampling campaign of the Silver Mine District, including a magnetic and/or gravitational anomaly study. Using the color changes and geochemical variation data above, heat maps can be developed to help identify previously undiscovered veins in the field area, including veins that may be up to ~10 m underground based on the horizontal color and geochemical changes. To test the applicability of this approach on a global scale, future research should apply a similar approach to comparable xenothermal polymetallic ore systems elsewhere.

# APPENDIX A.

# GRAVIMETRIC FIRE ASSAY DATA

| Sample ID | QC ID | Ag | Au |
|---|---|---|---|
| Units | | oz/ton | oz/ton |
| Detect Limit | | 0.1 | 0.016 |
| EEN0 | | <0.1 | <0.016 |
| EEN1 | | <0.1 | <0.016 |
| EEN2 | | <0.1 | <0.016 |
| EEN3 | | <0.1 | <0.016 |
| EEN4 | | <0.1 | <0.016 |
| EEN5 | | <0.1 | <0.016 |
| EEN6 | | <0.1 | <0.016 |
| EEN7 | | <0.1 | <0.016 |
| EEN8 | | <0.1 | <0.016 |
| EEN9 | | <0.1 | <0.016 |
| EES0 | | <0.1 | <0.016 |
| EES1 | | <0.1 | <0.016 |
| EES2 | | <0.1 | <0.016 |
| EES3 | | <0.1 | <0.016 |
| EES4 | | <0.1 | <0.016 |
| EES5 | | <0.1 | <0.016 |
| EES6 | | <0.1 | <0.016 |
| EES7 | | <0.1 | <0.016 |
| EES8 | | <0.1 | <0.016 |
| EES9 | | <0.1 | <0.016 |
| NDN0 | | <0.1 | <0.016 |
| NDN1 | | <0.1 | <0.016 |
| NDN2 | | <0.1 | <0.016 |
| NDN3 | | <0.1 | <0.016 |
| NDN4 | | <0.1 | <0.016 |
| NDN5 | | <0.1 | <0.016 |
| NDN6 | | <0.1 | <0.016 |
| NDN7 | | <0.1 | <0.016 |
| NDN8 | | <0.1 | <0.016 |
| NDN9 | | <0.1 | <0.016 |
| NDS0 | | <0.1 | <0.016 |
| NDS1 | | <0.1 | <0.016 |
| NDS2 | | <0.1 | <0.016 |
| NDS3 | | <0.1 | <0.016 |
| NDS4 | | <0.1 | <0.016 |
| NDS5 | | <0.1 | <0.016 |
| NDS6 | | <0.1 | <0.016 |
| NDS7 | | <0.1 | <0.016 |
| NDS8 | | <0.1 | <0.016 |
| NDS9 | | <0.1 | <0.016 |
| EEN1 | DUP | <0.1 | <0.016 |
| EES3 | DUP | <0.1 | <0.016 |
| NDN8 | DUP | <0.1 | <0.016 |

# APPENDIX B.

# MAJOR ELEMENT DATA

| Sample ID | QC ID | Al2O3 | BaO | CaO | Cr2O3 | Fe2O3 | K2O | MgO | MnO | Na2O | Nitrogen 105 | P2O5 | SiO2 | TiO2 | Total |
|---|---|---|---|---|---|---|---|---|---|---|---|---|---|---|---|
| Units | | wt% | wt% | wt% | wt% | wt% | wt% | wt% | wt% | wt% | wt% | wt% | wt% | wt% | wt% |
| Detect Limit | | | 0.02 | 0.004 | 0.006 | 0.002 | 0.01 | 0.01 | 0.01 | 0.002 | 0.02 | | 0.002 | 0.04 | 0.01 |
| EEN0 | | 16.35 | 0.058 | 1.396 | <0.002 | 5.56 | 4.86 | 0.64 | 0.299 | 0.18 | 0.34 | 0.082 | 64.99 | 0.33 | 97.32 |
| EEN1 | | 14.55 | 0.104 | 1.567 | <0.002 | 2.95 | 3.98 | 0.72 | 0.069 | 4.31 | 0.44 | 0.109 | 70.62 | 0.36 | 100.61 |
| EEN2 | | 14.44 | 0.094 | 1.689 | <0.002 | 3.08 | 3.92 | 0.7 | 0.08 | 4.36 | 0.26 | 0.115 | 70.71 | 0.37 | 100.44 |
| EEN3 | | 14.74 | 0.105 | 1.2 | 0.002 | 3.17 | 3.85 | 0.72 | 0.096 | 4.38 | 0.36 | 0.118 | 70.33 | 0.38 | 100.35 |
| EEN4 | | 14.39 | 0.102 | 1.589 | <0.002 | 3.09 | 3.9 | 0.68 | 0.074 | 4.27 | 0.48 | 0.115 | 69.95 | 0.37 | 99.82 |
| EEN5 | | 14.65 | 0.09 | 1.604 | <0.002 | 3.27 | 3.77 | 0.71 | 0.078 | 4.41 | 0.53 | 0.132 | 69.77 | 0.39 | 100.37 |
| EEN6 | | 14.52 | 0.103 | 0.702 | <0.002 | 3.05 | 3.94 | 0.57 | 0.063 | 4.33 | 0.74 | 0.127 | 70.18 | 0.38 | 99.98 |
| EEN7 | | 14.61 | 0.095 | 1.819 | <0.002 | 3.45 | 3.7 | 0.84 | 0.08 | 4.4 | 0.44 | 0.131 | 69.89 | 0.42 | 100.75 |
| EEN8 | | 14.76 | 0.108 | 1.657 | <0.002 | 3.05 | 3.9 | 0.67 | 0.069 | 4.36 | 0.37 | 0.113 | 70.62 | 0.36 | 100.81 |
| EEN9 | | 14.59 | 0.104 | 1.392 | <0.002 | 2.88 | 3.95 | 0.65 | 0.058 | 4.18 | 0.47 | 0.109 | 71.22 | 0.36 | 100.9 |
| EES0 | | 16.22 | 0.059 | 1.165 | 0.003 | 4.19 | 6.14 | 0.75 | 0.241 | 0.18 | 0.17 | 0.048 | 66.72 | 0.37 | 98.81 |
| EES1 | | 14.54 | 0.1 | 1.548 | <0.002 | 3.24 | 3.68 | 0.83 | 0.077 | 4.52 | 0.16 | 0.126 | 69.8 | 0.41 | 99.8 |
| EES2 | | 14.37 | 0.098 | 1.153 | 0.002 | 2.99 | 4.04 | 0.7 | 0.061 | 4.36 | 0.22 | 0.109 | 70.16 | 0.37 | 99.44 |
| EES3 | | 14.35 | 0.099 | 1.185 | <0.002 | 2.64 | 3.76 | 0.62 | 0.044 | 4.4 | 0.3 | 0.099 | 71.12 | 0.32 | 99.93 |
| EES4 | | 14.37 | 0.093 | 1.167 | <0.002 | 2.99 | 3.69 | 0.72 | 0.057 | 4.41 | 0.2 | 0.12 | 70.55 | 0.37 | 99.55 |
| EES5 | | 14.2 | 0.102 | 0.917 | <0.002 | 3.22 | 3.99 | 0.66 | 0.06 | 4 | 0.36 | 0.112 | 71.38 | 0.38 | 100.27 |
| EES6 | | 14.44 | 0.104 | 1.402 | <0.002 | 3.14 | 3.95 | 0.69 | 0.07 | 4.4 | 0.34 | 0.113 | 69.97 | 0.35 | 99.71 |
| EES7 | | 14.21 | 0.1 | 1.625 | <0.002 | 3.11 | 3.79 | 0.74 | 0.074 | 4.34 | 0.34 | 0.115 | 69.38 | 0.37 | 98.9 |
| EES8 | | 14.71 | 0.11 | 1.059 | <0.002 | 2.86 | 4.03 | 0.6 | 0.072 | 4.22 | 0.34 | 0.11 | 71.15 | 0.35 | 100.45 |
| EES9 | | 14.98 | 0.108 | 1.678 | 0.004 | 3.31 | 3.75 | 0.74 | 0.092 | 4.55 | 0.47 | 0.132 | 70.23 | 0.4 | 101.21 |
| NDN0 | | 14.39 | 0.069 | 3.166 | <0.002 | 4.27 | 5.58 | 0.91 | 0.267 | 0.14 | 0.41 | 0.108 | 65.58 | 0.36 | 98.39 |
| NDN1 | | 14.78 | 0.111 | 0.407 | <0.002 | 3.25 | 3.67 | 0.6 | 0.14 | 4.48 | 0.75 | 0.112 | 70.13 | 0.36 | 100.18 |
| NDN2 | | 14.59 | 0.096 | 1.197 | <0.002 | 2.79 | 3.84 | 0.58 | 0.063 | 4.31 | 0.68 | 0.103 | 70.94 | 0.33 | 100.48 |
| NDN3 | | 14.62 | 0.109 | 1.621 | <0.002 | 3.13 | 3.84 | 0.71 | 0.073 | 4.4 | 0.57 | 0.126 | 69.65 | 0.38 | 100.01 |
| NDN4 | | 14.6 | 0.096 | 1.382 | <0.002 | 3.13 | 3.83 | 0.66 | 0.071 | 4.23 | 0.74 | 0.134 | 70.06 | 0.38 | 100.25 |
| NDN5 | | 14.74 | 0.108 | 1.421 | <0.002 | 3.43 | 3.7 | 0.77 | 0.095 | 4.38 | 0.26 | 0.133 | 70.2 | 0.41 | 100.46 |
| NDN6 | | 14.49 | 0.101 | 1.272 | <0.002 | 3.16 | 3.86 | 0.65 | 0.094 | 4.36 | 0.54 | 0.134 | 69.78 | 0.38 | 99.81 |
| NDN7 | | 14.34 | 0.1 | 1.72 | <0.002 | 2.93 | 3.66 | 0.66 | 0.063 | 4.32 | 0.28 | 0.123 | 70.88 | 0.38 | 100.26 |
| NDN8 | | 14.59 | 0.093 | 1.452 | <0.002 | 2.86 | 3.49 | 0.72 | 0.06 | 4.48 | 0.34 | 0.123 | 71.17 | 0.38 | 100.6 |
| NDN9 | | 14.95 | 0.099 | 0.916 | <0.002 | 3.17 | 3.26 | 0.79 | 0.067 | 4.92 | 0.33 | 0.122 | 70.67 | 0.38 | 100.6 |
| NDS0 | | 13.85 | 0.057 | 1.874 | <0.002 | 4.28 | 4.93 | 0.59 | 0.305 | 0.15 | 0.43 | 0.06 | 69.36 | 0.33 | 98.33 |
| NDS1 | | 14.54 | 0.082 | 0.549 | <0.002 | 3.36 | 3.93 | 0.6 | 0.089 | 3.73 | 0.79 | 0.116 | 70.07 | 0.36 | 99.69 |
| NDS2 | | 14.38 | 0.1 | 1.637 | 0.002 | 3.12 | 4.12 | 0.63 | 0.115 | 4.25 | 0.29 | 0.111 | 70.37 | 0.36 | 100.05 |
| NDS3 | | 14.56 | 0.096 | 1.646 | <0.002 | 2.95 | 3.77 | 0.67 | 0.085 | 4.42 | 0.33 | 0.118 | 70.7 | 0.35 | 100.39 |
| NDS4 | | 14.51 | 0.093 | 1.812 | 0.002 | 3.33 | 3.55 | 0.75 | 0.085 | 4.49 | 0.32 | 0.131 | 69.47 | 0.4 | 99.72 |
| NDS5 | | 14.47 | 0.101 | 1.226 | <0.002 | 3.29 | 3.93 | 0.72 | 0.094 | 4.35 | 0.34 | 0.126 | 70.58 | 0.38 | 100.5 |
| NDS6 | | 14.54 | 0.098 | 0.589 | <0.002 | 3.11 | 3.86 | 0.62 | 0.104 | 4.59 | 0.27 | 0.119 | 69.76 | 0.38 | 99.14 |
| NDS7 | | 14.32 | 0.104 | 1.588 | <0.002 | 2.87 | 3.93 | 0.71 | 0.072 | 4.26 | 0.17 | 0.107 | 71.39 | 0.34 | 100.49 |
| NDS8 | | 14.69 | 0.099 | 1.744 | <0.002 | 3.23 | 3.8 | 0.79 | 0.077 | 4.48 | 0.32 | 0.125 | 70.42 | 0.38 | 100.79 |
| NDS9 | | 14.58 | 0.099 | 1.721 | 0.002 | 3.07 | 3.83 | 0.77 | 0.072 | 4.45 | 0.26 | 0.121 | 70.52 | 0.37 | 100.51 |
| EEN9 | DUP | 14.42 | 0.103 | 1.385 | <0.002 | 2.87 | 3.92 | 0.64 | 0.059 | 4.13 | 0.47 | 0.108 | 70.53 | 0.36 | 99.95 |
| EES9 | DUP | 14.8 | 0.11 | 1.665 | <0.002 | 3.3 | 3.77 | 0.74 | 0.093 | 4.52 | 0.47 | 0.131 | 69.45 | 0.4 | 100.22 |
| NDN9 | DUP | 14.92 | 0.099 | 0.921 | <0.002 | 3.18 | 3.26 | 0.78 | 0.068 | 4.9 | 0.35 | 0.123 | 70.62 | 0.37 | 100.53 |
| NDS6 | DUP | 14.65 | 0.096 | 0.585 | 0.002 | 3.1 | 3.88 | 0.63 | 0.102 | 4.6 | 0.29 | 0.12 | 70.46 | 0.39 | 99.97 |

# APPENDIX C.

# MINOR AND TRACE ELEMENT DATA

| Sample ID | QC ID | Ba | Be | Bi | Cd | Ce | Co | Cr | Cs | Cu | Dy | Er | Eu | Ga |
|---|---|---|---|---|---|---|---|---|---|---|---|---|---|---|
| Units | | ppm | ppm | ppm | ppm | ppm | ppm | ppm | ppm | ppm | ppm | ppm | ppm | ppm |
| Detect Limit | | 0.8 | 0.04 | 0.47 | 0.013 | 0.12 | 0.13 | 3 | 0.013 | 1.4 | 0.009 | 0.007 | 0.0031 | 0.04 |
| EEN0 | | 449.1 | 14.58 | 1.02 | >4 | 65.72 | 17.07 | <3 | 16.236 | 202.7 | 5.697 | 3.649 | 0.9486 | 17.85 |
| EEN1 | | 957 | 2.13 | <0.47 | 0.189 | 59.08 | 60.41 | <3 | 1.325 | 18.1 | 5.906 | 3.805 | 1.1854 | 16.14 |
| EEN2 | | 845.3 | 2.91 | <0.47 | 0.197 | 52.13 | 56.24 | 33 | 1.662 | 3.6 | 6.853 | 4.588 | 1.1938 | 16.68 |
| EEN3 | | 958.4 | 2.36 | <0.47 | 0.17 | 47.46 | 37.51 | 3 | 1.351 | 3.3 | 6.383 | 4.185 | 1.3268 | 16.37 |
| EEN4 | | 923.6 | 2.29 | <0.47 | 0.105 | 57.71 | 58.87 | 3 | 1.538 | 3.3 | 5.785 | 3.822 | 1.1304 | 16.16 |
| EEN5 | | 789.6 | 2.97 | <0.47 | 0.147 | 76.74 | 52.35 | 3 | 1.734 | 3 | 6.3 | 4.124 | 1.1602 | 17.07 |
| EEN6 | | 931.5 | 10.4 | <0.47 | 0.146 | 59.18 | 57.71 | 3 | 2.175 | 6.4 | 4.966 | 3.169 | 1.1724 | 16.83 |
| EEN7 | | 854.5 | 2.11 | <0.47 | 0.103 | 60.15 | 37.45 | 3 | 1.856 | 2.8 | 7.049 | 4.67 | 1.2617 | 16.64 |
| EEN8 | | 988.8 | 2.38 | <0.47 | 0.116 | 71.26 | 30.6 | <3 | 1.494 | 1.8 | 5.923 | 3.856 | 1.2104 | 16.47 |
| EEN9 | | 958.1 | 2.13 | <0.47 | 0.092 | 49.89 | 44 | <3 | 1.471 | 1.8 | 4.778 | 3.176 | 1.1351 | 16.39 |
| EES0 | | 497.6 | 27.15 | 8.73 | 0.253 | 64.28 | 11.47 | <3 | 14.163 | 19.1 | 5.112 | 3.507 | 0.7977 | 18.32 |
| EES1 | | 873.5 | 2.21 | <0.47 | 0.094 | 63.06 | 28.74 | <3 | 1.502 | 1.7 | 7.44 | 4.994 | 1.2529 | 16.1 |
| EES2 | | 881.9 | 3.17 | <0.47 | 0.157 | 54.67 | 33.71 | 3 | 1.8 | 2.6 | 6.263 | 3.998 | 1.3401 | 16.32 |
| EES3 | | 898.3 | 3.22 | <0.47 | 0.079 | 67.25 | 31.69 | <3 | 2.042 | 3 | 5.711 | 3.623 | 1.2099 | 16.01 |
| EES4 | | 844.8 | 2.75 | <0.47 | 0.064 | 67.02 | 30.74 | <3 | 1.733 | 1.4 | 7.343 | 4.723 | 1.3282 | 16.25 |
| EES5 | | 899.6 | 2.13 | <0.47 | 0.085 | 54.63 | 61.57 | 4 | 1.639 | 2.8 | 5.84 | 3.931 | 1.1323 | 16.22 |
| EES6 | | 954.7 | 2.14 | <0.47 | 0.103 | 67.95 | 50.93 | 5 | 1.135 | 4.9 | 5.911 | 3.885 | 1.213 | 16.72 |
| EES7 | | 904.7 | 2.71 | <0.47 | 0.119 | 70.91 | 28.21 | 4 | 1.805 | 4 | 8.408 | 5.112 | 1.5625 | 16.71 |
| EES8 | | 1013.7 | 2.15 | <0.47 | 0.083 | 66.05 | 26.92 | 3 | 1.3 | 5.9 | 5.928 | 3.931 | 1.1843 | 16.57 |
| EES9 | | 997.8 | 1.87 | <0.47 | 0.121 | 59.02 | 60.76 | 3 | 1.38 | 2.3 | 6.482 | 4.236 | 1.2735 | 17.05 |
| NDN0 | | 598.6 | 15.99 | 1.75 | 0.218 | 70.55 | 30.64 | 4 | 22.343 | 66.3 | 5.696 | 3.816 | 1.3018 | 21.55 |
| NDN1 | | 1035.9 | 2.87 | <0.47 | 0.164 | 42.27 | 79.32 | <3 | 1.879 | 8.3 | 3.617 | 2.672 | 0.8195 | 16.66 |
| NDN2 | | 895.7 | 2.44 | <0.47 | 0.097 | 96.46 | 80.87 | 11 | 1.444 | 2.5 | 5.945 | 3.825 | 1.3162 | 16.82 |
| NDN3 | | 1017.5 | 2.01 | <0.47 | 0.107 | 73.05 | 68.5 | 41 | 1.252 | 3.1 | 6.832 | 4.509 | 1.2913 | 16.77 |
| NDN4 | | 839.3 | 2.33 | <0.47 | 0.125 | 71.61 | 103.92 | 3 | 1.688 | 2.3 | 6.875 | 4.489 | 1.282 | 16.54 |
| NDN5 | | 962.1 | 1.95 | <0.47 | 0.113 | 67.24 | 36.32 | 3 | 1.633 | 4 | 6.486 | 4.219 | 1.288 | 17.03 |
| NDN6 | | 922 | 2.53 | <0.47 | 0.114 | 78.4 | 58.5 | 3 | 1.884 | 2.2 | 7.35 | 4.804 | 1.3128 | 16.73 |
| NDN7 | | 909.3 | 2.04 | <0.47 | 0.105 | 67.04 | 41.02 | 3 | 1.079 | 4.4 | 6.293 | 4.157 | 1.2067 | 16.41 |
| NDN8 | | 847.3 | 2.26 | <0.47 | 0.103 | 99.07 | 30.06 | 3 | 1.255 | 1.7 | 6.77 | 4.353 | 1.2918 | 16.59 |
| NDN9 | | 904.9 | 2.07 | <0.47 | 0.235 | 61.72 | 47.38 | 3 | 1.313 | 32 | 6.165 | 4.101 | 1.2319 | 16.73 |
| NDS0 | | 484.7 | 12.87 | 4.31 | >4 | 71.07 | 28.75 | 4 | 19.383 | 75.2 | 5.918 | 3.895 | 1.0798 | 20.23 |
| NDS1 | | 759.7 | 6.92 | <0.47 | 0.345 | 52.21 | 28.73 | 5 | 3.866 | 27.3 | 6.16 | 3.971 | 1.1149 | 16.11 |
| NDS2 | | 917.2 | 1.8 | <0.47 | 0.216 | 63 | 34.82 | 5 | 1.65 | 7.6 | 5.904 | 3.774 | 1.2079 | 16.61 |
| NDS3 | | 894.9 | 2.23 | <0.47 | 0.203 | 62.67 | 45.56 | 3 | 1.99 | 2.4 | 6.258 | 4.232 | 1.2174 | 16.92 |
| NDS4 | | 865.5 | 2.02 | <0.47 | 0.124 | 68.56 | 40.58 | 3 | 1.574 | 4.4 | 6.67 | 4.336 | 1.2788 | 17.07 |
| NDS5 | | 933.4 | 3.55 | <0.47 | 0.175 | 74.64 | 33.59 | 3 | 1.553 | 4 | 7.701 | 4.988 | 1.3277 | 16.68 |
| NDS6 | | 872.4 | 8.08 | <0.47 | 0.14 | 68.12 | 26.68 | 3 | 1.809 | 82.1 | 5.018 | 3.298 | 1.2277 | 16.66 |
| NDS7 | | 945.4 | 1.89 | <0.47 | 0.243 | 76.7 | 30.3 | 3 | 1.871 | 6 | 5.972 | 3.916 | 1.1867 | 16.42 |
| NDS8 | | 891.8 | 2.23 | <0.47 | 0.134 | 63.23 | 54.76 | 4 | 1.463 | 3.7 | 6.208 | 4.192 | 1.186 | 16.77 |
| NDS9 | | 913.9 | 1.76 | <0.47 | 0.101 | 65.36 | 51.88 | <3 | 1.361 | 4.9 | 6.056 | 3.956 | 1.2006 | 16.38 |
| EEN0 | DUP | 426.8 | 12.61 | 0.99 | >4 | 67.61 | 17.18 | <3 | 16.401 | 204.8 | 5.502 | 3.629 | 0.9217 | 18.34 |
| EES0 | DUP | 504.1 | 26.67 | 8.71 | 0.132 | 73.81 | 11.6 | <3 | 14.261 | 19.1 | 5.643 | 3.847 | 0.8431 | 18.57 |
| NDN0 | DUP | 591.7 | 15.43 | 1.78 | 0.229 | 69.43 | 29.73 | 3 | 21.723 | 64.8 | 5.888 | 3.942 | 1.3031 | 21.23 |
| NDS0 | DUP | 468.5 | 12 | 4.25 | >4 | 73.3 | 27.85 | 4 | 19.043 | 74.2 | 5.736 | 3.827 | 1.0557 | 19.85 |

| Gd | Hf | Ho | In | La | Li | Lu | Mo | Nb | Nd | Ni | Pb | Pr | Rb | Sb | Sc |
|---|---|---|---|---|---|---|---|---|---|---|---|---|---|---|---|
| ppm | ppm | ppm | ppm | ppm | ppm | ppm | ppm | ppm | ppm | ppm | ppm | ppm | ppm | ppm | ppm |
| 0.009 | 0.14 | 0.0025 | 0.0018 | 0.1 | 0.4 | 0.002 | 0.08 | 0.028 | 0.06 | 0.7 | 0.18 | 0.014 | 0.11 | 0.04 | 1.1 |
| 5.725 | 5.53 | 1.2003 | >1.9 | 33.3 | >207 | 0.603 | 2.17 | 7.31 | 34.64 | 1.7 | >700 | 8.882 | 1160.25 | 0.96 | 6.2 |
| 5.654 | 5.89 | 1.2601 | 0.0649 | 30.3 | 24.9 | 0.625 | 0.45 | 8.269 | 30.51 | 1.6 | 14.63 | 7.845 | 116.8 | 0.13 | 7.1 |
| 6.262 | 6.32 | 1.4515 | 0.058 | 29.1 | 15 | 0.746 | 0.54 | 9.481 | 30.66 | 2.1 | 15.8 | 7.619 | 119.05 | 0.18 | 8 |
| 6.028 | 5.92 | 1.3607 | 0.0556 | 25 | 25.4 | 0.678 | 0.6 | 8.641 | 27.75 | 1.9 | 18.46 | 6.706 | 120.82 | 0.32 | 7.8 |
| 5.48 | 6.1 | 1.2376 | 0.0507 | 26.3 | 19.8 | 0.651 | 0.4 | 8.709 | 28.09 | 2.5 | 9.78 | 7.055 | 116.82 | 0.15 | 8 |
| 5.713 | 6.29 | 1.312 | 0.054 | 29.8 | 18.2 | 0.687 | 1.43 | 9.558 | 29.72 | 2.1 | 14.86 | 7.754 | 127.7 | 0.31 | 8.7 |
| 5.237 | 5.62 | 1.0303 | 0.079 | 28.7 | 26.3 | 0.548 | 0.94 | 8.659 | 30.22 | 1.7 | 17.28 | 7.632 | 173.89 | 0.2 | 8.5 |
| 6.564 | 6.19 | 1.4871 | 0.0698 | 28.1 | 21 | 0.751 | 0.52 | 9.319 | 31.5 | 1.6 | 9.84 | 7.699 | 107.84 | 0.2 | 9.3 |
| 5.497 | 5.44 | 1.2439 | 0.0545 | 23.5 | 12.1 | 0.632 | 0.63 | 8.174 | 26.98 | 1.9 | 8.38 | 6.855 | 108.43 | 0.13 | 7.7 |
| 4.418 | 5.76 | 1.016 | 0.0487 | 19.8 | 13.4 | 0.531 | 0.39 | 8.304 | 22.83 | 2.2 | 10.09 | 5.618 | 109.41 | 0.11 | 7.7 |
| 4.383 | 5.74 | 1.116 | 1.394 | 32.3 | >207 | 0.593 | 1.04 | 8.396 | 31.92 | 1 | 224.22 | 8.062 | 1385.91 | 0.48 | 7.5 |
| 7.032 | 6.24 | 1.6068 | 0.0631 | 31.1 | 26.2 | 0.816 | 0.55 | 9.528 | 33.76 | 1.5 | 11.15 | 8.309 | 119.13 | 0.19 | 8.4 |
| 6.384 | 5.46 | 1.3137 | 0.0563 | 30.9 | 30 | 0.64 | 0.97 | 8.691 | 32.1 | 3.3 | 9.02 | 8.004 | 139.91 | 0.2 | 8.2 |
| 6.02 | 5.54 | 1.1691 | 0.0497 | 36.6 | 27.5 | 0.588 | 0.53 | 7.856 | 33.66 | 1.9 | 5.94 | 8.781 | 106.61 | 0.15 | 6.9 |
| 7.319 | 5.92 | 1.5615 | 0.0554 | 40.4 | 22 | 0.762 | 0.43 | 9.024 | 37.88 | 1.3 | 6.74 | 9.719 | 103.89 | 0.18 | 7.9 |
| 5.596 | 5.95 | 1.2473 | 0.0528 | 30.9 | 22.2 | 0.67 | 0.61 | 9.39 | 32 | 2.2 | 8.83 | 8.17 | 111.22 | 0.23 | 8.6 |
| 5.837 | 5.48 | 1.2687 | 0.0613 | 33.4 | 16.9 | 0.63 | 0.69 | 8.522 | 32.36 | 3.1 | 10.56 | 8.371 | 110.17 | 0.18 | 7.7 |
| 8.658 | 5.79 | 1.7443 | 0.0567 | 48 | 20 | 0.825 | 0.88 | 8.746 | 45.72 | 2.6 | 8.83 | 11.542 | 110.91 | 0.17 | 8.2 |
| 5.58 | 5.84 | 1.2705 | 0.0476 | 29.9 | 11.9 | 0.669 | 0.51 | 8.269 | 30.16 | 1.8 | 10.31 | 7.742 | 104.94 | 0.18 | 7.3 |
| 6.361 | 6.06 | 1.4016 | 0.0572 | 36 | 15.3 | 0.696 | 0.49 | 9.402 | 34.85 | 1.8 | 10.75 | 8.824 | 108.6 | 0.1 | 8.6 |
| 5.655 | 5.41 | 1.2394 | 0.589 | 41.3 | >207 | 0.661 | 0.33 | 8.999 | 36.65 | 2.4 | 480.55 | 9.364 | 1497.98 | 0.45 | 9.1 |
| 3.437 | 5.92 | 0.7976 | 0.0328 | 20.7 | 36.9 | 0.528 | 1.13 | 8.093 | 21.37 | 2.6 | 14.12 | 5.445 | 180.77 | 0.19 | 7 |
| 5.995 | 5.73 | 1.2231 | 0.0493 | 37.8 | 21.1 | 0.641 | 1.01 | 8.658 | 37.19 | 3 | 11.31 | 9.837 | 122.76 | 0.28 | 7.4 |
| 6.653 | 6.26 | 1.4577 | 0.0499 | 35.6 | 17.4 | 0.751 | 0.49 | 8.79 | 35.16 | 2.5 | 12.62 | 9.186 | 114.06 | 0.17 | 8 |
| 6.505 | 6.09 | 1.445 | 0.0492 | 32.3 | 19.9 | 0.74 | 0.32 | 8.761 | 34.58 | 2.2 | 12.64 | 8.857 | 115.21 | 0.2 | 8.2 |
| 6.216 | 5.93 | 1.3797 | 0.057 | 31.8 | 32.1 | 0.687 | 0.36 | 9.056 | 33.3 | 1.5 | 16.42 | 8.338 | 109.85 | 0.23 | 9 |
| 7.18 | 6.21 | 1.5845 | 0.0472 | 38.5 | 18 | 0.78 | 0.43 | 9.07 | 38 | 1.9 | 13.68 | 9.777 | 137.96 | 0.33 | 8.1 |
| 6.072 | 6.12 | 1.331 | 0.0506 | 33.4 | 16.7 | 0.687 | 0.39 | 8.792 | 32.75 | 1.4 | 16.44 | 8.357 | 96.81 | 0.14 | 8.6 |
| 6.907 | 6 | 1.4146 | 0.0598 | 47.5 | 18.5 | 0.728 | 0.39 | 9.188 | 43.91 | 1.5 | 13.47 | 11.803 | 90.18 | 0.13 | 8.5 |
| 5.81 | 5.76 | 1.331 | 0.0624 | 28 | 18.2 | 0.679 | 0.4 | 8.7 | 30.1 | 2.2 | 41.77 | 7.723 | 95.03 | 0.2 | 8.2 |
| 5.592 | 5.38 | 1.2578 | 1.4914 | 35.4 | >207 | 0.634 | 1.53 | 7.733 | 31.97 | 2.2 | 391.96 | 8.607 | 1423.56 | 0.45 | 8.4 |
| 5.745 | 5.65 | 1.3173 | 0.2363 | 25 | 125.9 | 0.667 | 1 | 8.052 | 27.48 | 4 | 43.42 | 6.759 | 218.92 | 0.48 | 6.7 |
| 5.677 | 5.74 | 1.2416 | 0.051 | 29.8 | 16.9 | 0.635 | 19.21 | 8.474 | 30.36 | 3.3 | 27.65 | 7.751 | 128.01 | 0.26 | 8.1 |
| 5.849 | 5.96 | 1.3412 | 0.0454 | 30 | 26.5 | 0.701 | 0.87 | 8.972 | 30.11 | 2.5 | 15.13 | 7.742 | 119.24 | 0.19 | 7.6 |
| 6.363 | 5.94 | 1.3944 | 0.0521 | 32 | 19.5 | 0.695 | 0.41 | 9.073 | 33.71 | 1.9 | 12.16 | 8.54 | 116.43 | 0.23 | 8.9 |
| 7.331 | 6.15 | 1.6244 | 0.0427 | 39.6 | 32.3 | 0.843 | 1.47 | 9.337 | 37.96 | 2.5 | 20.46 | 9.717 | 155.04 | 0.31 | 8.4 |
| 5.272 | 5.7 | 1.0387 | 0.0362 | 37.7 | 41.9 | 0.573 | 2.64 | 8.71 | 33.76 | 2.2 | 478.37 | 8.893 | 190.85 | 0.33 | 8.2 |
| 5.964 | 5.47 | 1.2677 | 0.0462 | 38.2 | 32.2 | 0.634 | 0.89 | 7.853 | 35.9 | 1.5 | 17.7 | 9.413 | 113.81 | 0.17 | 8 |
| 5.965 | 6.11 | 1.3417 | 0.0566 | 30.3 | 19.7 | 0.69 | 0.5 | 8.915 | 31 | 2.3 | 13.67 | 7.909 | 109.78 | 0.18 | 8.3 |
| 5.927 | 5.92 | 1.2943 | 0.0614 | 32.3 | 10.7 | 0.642 | 0.57 | 7.883 | 31.79 | 2 | 11.91 | 8.069 | 100.26 | 0.13 | 7.8 |
| 5.62 | 5.7 | 1.1539 | >1.9 | 33.2 | >207 | 0.583 | 2.01 | 7.565 | 34.34 | 1.7 | >700 | 8.777 | 1122.53 | 0.95 | 5.5 |
| 4.882 | 6.01 | 1.2297 | 1.4222 | 37.1 | >207 | 0.635 | 0.84 | 8.495 | 35.39 | 1 | 221.74 | 9.183 | 1404.4 | 0.48 | 7.8 |
| 5.627 | 5.58 | 1.2404 | 0.5904 | 40.6 | >207 | 0.672 | 0.35 | 8.79 | 36.4 | 2.2 | 484.31 | 9.201 | 1403.32 | 0.45 | 8.4 |
| 5.653 | 5.35 | 1.2425 | 1.4649 | 35.4 | >207 | 0.642 | 1.48 | 7.627 | 32.11 | 2.3 | 383.57 | 8.747 | 1379.67 | 0.43 | 8.1 |

| Sm | Sn | Sr | Ta | Tb | Th | Ti | Tl | Tm | U | V | W | Y | Yb | Zn | Zr |
|---|---|---|---|---|---|---|---|---|---|---|---|---|---|---|---|
| ppm | ppm | ppm | ppm | ppm | ppm | ppm | ppm | ppm | ppm | ppm | ppm | ppm | ppm | ppm | ppm |
| 0.026 | 0.16 | 0.6 | 0.007 | 0.0023 | 0.018 | 7 | 0.002 | 0.0019 | 0.011 | 0.8 | 0.05 | 0.05 | 0.009 | 1.8 | 6 |
| 6.857 | >14 | 45 | 0.624 | 0.9016 | 6.996 | 1884 | 3.972 | 0.5688 | 2.599 | 20.5 | >141 | 34.58 | 3.866 | 7805.6 | 179 |
| 6.214 | 2.26 | 168.4 | 0.623 | 0.9084 | 8.155 | 2051 | 0.369 | 0.5836 | 1.83 | 20.1 | >141 | 35.31 | 4.049 | 59.6 | 201 |
| 6.647 | 1.74 | 164.4 | 0.879 | 1.0253 | 9.093 | 2106 | 0.376 | 0.6948 | 2.49 | 24.3 | >141 | 41.05 | 4.796 | 70.1 | 201 |
| 6.21 | 1.86 | 175.6 | 0.607 | 0.9871 | 6.867 | 2225 | 0.431 | 0.6373 | 1.845 | 23.8 | >141 | 39.38 | 4.383 | 64.9 | 206 |
| 5.977 | 2.3 | 177.3 | 0.664 | 0.8889 | 7.528 | 2134 | 0.381 | 0.6009 | 1.654 | 21.9 | >141 | 34.66 | 4.106 | 37.7 | 211 |
| 6.305 | 2.56 | 169.1 | 0.739 | 0.9367 | 8.534 | 2245 | 0.421 | 0.6214 | 2.163 | 24.3 | >141 | 36.92 | 4.358 | 53.9 | 211 |
| 6.036 | 3.49 | 159.6 | 0.644 | 0.7877 | 7.444 | 2332 | 0.666 | 0.4988 | 2.532 | 24.3 | >141 | 29.1 | 3.451 | 357.4 | 201 |
| 6.826 | 2.54 | 168.1 | 0.669 | 1.0682 | 7.359 | 2394 | 0.357 | 0.7042 | 2.021 | 28.9 | >141 | 41.85 | 4.861 | 40.1 | 214 |
| 5.97 | 1.86 | 176.9 | 0.595 | 0.9022 | 7.688 | 2114 | 0.331 | 0.5923 | 2.419 | 23.9 | >141 | 34.56 | 4.127 | 29.7 | 189 |
| 4.902 | 1.88 | 172.1 | 0.611 | 0.7391 | 6.631 | 2106 | 0.33 | 0.4805 | 1.951 | 21.8 | >141 | 27.52 | 3.394 | 32.3 | 203 |
| 6.194 | >14 | 192.8 | 0.625 | 0.7418 | 6.542 | 2149 | 4.228 | 0.5478 | 2.52 | 24.1 | >141 | 31.5 | 3.767 | 106.3 | 192 |
| 7.318 | 3.11 | 169.8 | 0.706 | 1.1135 | 9.28 | 2339 | 0.431 | 0.7625 | 2.02 | 24.7 | >141 | 46.38 | 5.267 | 37.3 | 212 |
| 6.79 | 2.29 | 157.6 | 0.576 | 0.9949 | 7.274 | 2288 | 0.52 | 0.6056 | 1.806 | 25.2 | >141 | 37.37 | 4.093 | 78.4 | 196 |
| 6.619 | 2.6 | 143.8 | 0.601 | 0.9241 | 8.294 | 1938 | 0.328 | 0.5434 | 1.726 | 21 | >141 | 34.84 | 3.766 | 34.9 | 188 |
| 7.63 | 1.84 | 147.9 | 0.685 | 1.1527 | 7.81 | 2193 | 0.327 | 0.7002 | 1.956 | 23.6 | >141 | 43.69 | 4.855 | 36 | 199 |
| 6.425 | 2.21 | 162.8 | 0.687 | 0.8806 | 9.132 | 2239 | 0.398 | 0.6207 | 2.009 | 24.6 | >141 | 33.27 | 4.333 | 41.4 | 208 |
| 6.555 | 1.86 | 174.5 | 0.591 | 0.9222 | 7.443 | 2129 | 0.333 | 0.5783 | 1.69 | 23.2 | >141 | 36.3 | 4.031 | 40.8 | 195 |
| 9.337 | 1.7 | 159.7 | 0.578 | 1.3395 | 7.86 | 2225 | 0.329 | 0.7804 | 1.898 | 25 | >141 | 48.27 | 5.276 | 68.2 | 205 |
| 6.131 | 1.91 | 167 | 0.644 | 0.8999 | 7.791 | 2047 | 0.368 | 0.6183 | 2.011 | 21.1 | >141 | 35.17 | 4.31 | 38 | 196 |
| 6.921 | 1.4 | 181.4 | 0.565 | 1.0181 | 5.751 | 2347 | 0.319 | 0.65 | 1.5 | 24.8 | >141 | 39.56 | 4.512 | 43.5 | 223 |
| 7.702 | >14 | 126.8 | 0.631 | 0.8771 | 8.571 | 2096 | 3.841 | 0.6015 | 2.792 | 26.1 | >141 | 39.65 | 4.215 | 230.7 | 186 |
| 4.197 | 3.04 | 146.1 | 0.601 | 0.5347 | 6.763 | 2099 | 0.77 | 0.4406 | 1.858 | 22 | >141 | 20.04 | 3.297 | 97.2 | 201 |
| 7.247 | 2.06 | 171.9 | 0.715 | 0.9405 | 8.757 | 1989 | 0.39 | 0.5924 | 2.365 | 22.5 | >141 | 32.7 | 4.217 | 60.1 | 193 |
| 7.172 | 2.28 | 188.8 | 0.633 | 1.0535 | 7.781 | 2252 | 0.349 | 0.6976 | 1.896 | 24.7 | >141 | 41.39 | 4.782 | 33.2 | 219 |
| 7.346 | 2.29 | 165.1 | 0.623 | 1.0773 | 7.631 | 2229 | 0.357 | 0.6932 | 1.773 | 23.9 | >141 | 39.07 | 4.772 | 40.9 | 215 |
| 7.029 | 1.85 | 198.5 | 0.622 | 0.9983 | 7.605 | 2366 | 0.348 | 0.6504 | 1.644 | 26.7 | >141 | 38.62 | 4.402 | 51.5 | 210 |
| 7.758 | 2.62 | 179.7 | 0.678 | 1.1449 | 8.525 | 2262 | 0.452 | 0.7342 | 1.944 | 23.2 | >141 | 44.73 | 5.06 | 40.4 | 218 |
| 6.634 | 2.7 | 206.9 | 0.622 | 0.9739 | 7.938 | 2256 | 0.325 | 0.6366 | 1.851 | 25.3 | >141 | 38.23 | 4.419 | 33.1 | 216 |
| 8.215 | 3.91 | 184.6 | 0.66 | 1.0603 | 9.064 | 2281 | 0.305 | 0.676 | 2.011 | 25.2 | >141 | 40.27 | 4.629 | 37.7 | 209 |
| 6.483 | 3.27 | 249.9 | 0.616 | 0.9456 | 6.394 | 2208 | 0.304 | 0.636 | 1.842 | 24 | >141 | 36.13 | 4.405 | 83.3 | 202 |
| 6.363 | >14 | 51.4 | 0.574 | 0.9084 | 7.092 | 2003 | 4.052 | 0.6087 | 2.399 | 21.8 | >141 | 36.46 | 4.139 | 2376.2 | 182 |
| 6.015 | 2.77 | 123.6 | 0.583 | 0.9495 | 7.785 | 2065 | 0.833 | 0.6256 | 2.249 | 22.1 | >141 | 36.33 | 4.336 | 419.5 | 191 |
| 6.357 | 1.97 | 181.8 | 0.605 | 0.9137 | 7.253 | 2166 | 0.4 | 0.5834 | 2.74 | 23.7 | >141 | 35.92 | 4.014 | 58 | 205 |
| 6.389 | 2.1 | 176.9 | 0.698 | 0.9388 | 8.673 | 2083 | 0.353 | 0.6416 | 2.392 | 21 | >141 | 38.38 | 4.517 | 56.5 | 205 |
| 7.007 | 2.59 | 188.5 | 0.612 | 1.0288 | 7.943 | 2406 | 0.354 | 0.661 | 1.952 | 25.8 | >141 | 39.03 | 4.537 | 60.1 | 211 |
| 7.75 | 3.3 | 160.9 | 0.653 | 1.1714 | 8.81 | 2274 | 0.55 | 0.7866 | 2.129 | 24.4 | >141 | 43.89 | 5.493 | 83.4 | 213 |
| 6.475 | 3.28 | 114.9 | 0.598 | 0.7867 | 7.525 | 2278 | 0.666 | 0.5211 | 2.235 | 23.5 | >141 | 27.76 | 3.736 | 162 | 204 |
| 6.659 | 1.78 | 171 | 0.55 | 0.9108 | 7.743 | 2099 | 0.33 | 0.5931 | 1.817 | 22.7 | >141 | 37.39 | 3.974 | 44.5 | 199 |
| 6.459 | 1.77 | 183.6 | 0.64 | 0.9661 | 8.122 | 2245 | 0.315 | 0.6369 | 2.336 | 24.7 | >141 | 38.79 | 4.465 | 42.2 | 217 |
| 6.482 | 1.82 | 170.1 | 0.562 | 0.9419 | 7.79 | 2068 | 0.323 | 0.6096 | 2.001 | 23.2 | >141 | 35.46 | 4.146 | 33.1 | 202 |
| 6.845 | >14 | 45.3 | 0.628 | 0.8806 | 7.547 | 1896 | 3.953 | 0.5514 | 2.806 | 20.9 | >141 | 33.91 | 3.787 | 7907.6 | 186 |
| 6.714 | >14 | 193.3 | 0.626 | 0.822 | 6.896 | 2197 | 4.183 | 0.5894 | 2.586 | 23.4 | >141 | 34.08 | 4.147 | 108 | 201 |
| 7.593 | >14 | 123.2 | 0.638 | 0.886 | 8.568 | 2061 | 3.931 | 0.6053 | 2.81 | 25.3 | >141 | 38.97 | 4.247 | 225.2 | 187 |
| 6.285 | >14 | 50.3 | 0.576 | 0.888 | 6.899 | 1971 | 4.019 | 0.5835 | 2.327 | 21.8 | >141 | 35.76 | 4.091 | 2343.2 | 181 |

## REFERENCES


Balogh, S. K., K. L. Shelton, R. D. Hagni, G. Kisvarsanyi, and S. K. Grant. "Sulfur isotope and minor element geochemistry of the silver-tungsten-tin ore deposits in the Silver Mine district, Missouri." In *North American conference on tectonic control of ore deposits and the vertical and horizontal extent of ore systems. Proceedings volume: Rolla, University of Missouri-Rolla*, pp. 386-395. 1988.

Bickford, Marion Eugene, and D. G. Mose. *Geochronology of Precambrian rocks in the St. Francois Mountains, southeastern Missouri*. Vol. 165. Geological Society of America, 1975.

Bickford, M. E. "Geochronological studies in the St. Francois mountains, Missouri. "*Studies in Precambrian geology of Missouri: Missouri Geological Survey Report of Investigation* 61 (1976): 149-154.

Bickford, M. E., W. R. Van Schmus, K. E. Karlstrom, P. A. Mueller, and G. D. Kamenov. "Mesoproterozoic-trans-Laurentian magmatism: A synthesis of continent-wide age distributions, new SIMS U–Pb ages, zircon saturation temperatures, and Hf and Nd isotopic compositions." *Precambrian Research* 265 (2015): 286-312.

Buddington, A.F., 1935. High-temperature mineral associations at shallow to moderate depths. *Economic Geology*, *30*(3), pp. 205-222.

Collins, Earl M., and Stephen E. Kesler. "High temperature telescoped tungsten-antimony mineralization, Guatemala." *Mineralium Deposita* 4, no. 1 (1969): 65-71.

Gallego Hernandez, Alba Nury, and Masahide Akasaka. "Silver-bearing and associated minerals in El Zancudo deposit, Antioquia, Colombia." *Resource geology* 57, no. 4 (2007): 386-399.

Guilbert, J. M., and C. F. Park Jr. "The Geology of Ore Deposits, Freeman and Company." *New York* 985 (1986).

Hagni, Richard D. "Precambrian Silver-Tungsten-Tin Mineralization and Its Relationship to Granitic Magmatism in Southeastern Missouri, USA." (1982): 345.

Hagni, Richard D. "Ore microscopy of the silver minerals in the epigenetic Ag-W-Sn deposits in the Silver Mine district, southeastern Missouri, USA." In *Syngenesis and Epigenesis in the Formation of Mineral Deposits*, pp. 52-61. Springer, Berlin, Heidelberg, 1984.

Howe, Wallace Brady, and John W. Koenig. *The Stratigraphic Succession in Missouri*. Rolla, MO: Missouri Dept. of Natural Resources, Division of Geology and Land Survey, 1995.

Imai, Hideki, Min Sung Lee, Kohei Iida, Yoshinori Fujiki, and S. Takenouchi. "Geologic structure and mineralization of the xenothermal vein-type deposits in Japan." *Economic Geology* 70, no. 4 (1975): 647-676.

Kisvarsanyi, Eva B., and Arthur W. Hebrank. "Silver Mine district: Precambrian Ag-W-Pb mineralization and granite shut-ins, the St. Francois Mountains, Missouri." *North-Central Section of the Geological Society of America: Decade of North American Geology, Centennial Field Guide Volume 3* 3 (1987): 165.

Kisvarsanyi, Eva B. "Precambrian Rocks and Ore Deposits in the St. Francois Mountains, Southeast Missouri--A Middle Proterozoic Terrane of Granite Ring Complexes and Associated Rhyolites." *Precambrian and Paleozoic Geology and Ore Deposits in the Midcontinent Region: Rosiclare, Illinois to Ironton and Viburnum, Missouri June 30–July 8, 1989* 147 (1989): 37-50.

Large, Ross R., Jocelyn McPhie, J. Bruce Gemmell, Walter Herrmann, and Garry J. Davidson. "The spectrum of ore deposit types, volcanic environments, alteration halos, and related exploration vectors in submarine volcanic successions: Some examples from Australia." *Economic Geology* 96, no. 5 (2001): 913-938.

Lee, Min Sung, Sukune Takenouchi, and Hideki Imai. "Syntheses of stannoidite and mawsonite and their genesis in ore deposits." *Economic Geology* 70, no. 4 (1975): 834-843.

Leonard, Benjamin Franklin, Cynthia W. Mead, and Nancy Conklin. *Silver-rich disseminated sulfides from a tungsten-bearing quartz lode, Big Creek district, central Idaho*. No. 594-C. 1968.

Lofstrom, Dotty Mae. "Fluid inclusion and stable isotope studies of the Silver Mine District Sn-W-Pb-Zn-Ag deposits, Southeast Missouri." PhD diss., University Missouri-Columbia, 1987.

Lowell, G. R. "Precambrian geology and ore deposits of the Silver Mine area, southeast Missouri: a review." *A Field Guide to the Precambrian Geology of the St. Francois Mountains, Missouri. Big Rivers Area Geological Society* (1976): 81-88.

Lowell, G. R., and C. Gasparrini. "Composition of arsenopyrite from topaz greisen veins in Southeastern Missouri." *Mineralium Deposita* 17, no. 2 (1982): 229-238.

Lowell, Gary R. "The Butler Hill Caldera: a mid-Proterozoic ignimbrite-granite complex." *Precambrian Research* 51, no. 1-4 (1991): 245-263.

Lowell, G. R., and G. J. Young. "Interaction between coeval mafic and felsic melts in the St. Francois Terrane of Missouri, USA." *Precambrian Research* 95, no. 1-2 (1999): 69-88.

McDonough, William F., and S-S. Sun. "The composition of the Earth." *Chemical geology* 120, no. 3-4 (1995): 223-253.

Middlemost, E.A.K., 1994. Naming materials in the magma/igneous rock system. Earth-Science Reviews 37, 215–224.

Moon, Charles J., Michael KG Whateley, and Anthony M. Evans. *Introduction to mineral exploration*. No. Ed. 2. Blackwell publishing, 2006.

Pour, Amin Beiranvnd, and Mazlan Hashim. "Identification of hydrothermal alteration minerals for exploring of porphyry copper deposit using ASTER data, SE Iran." *Journal of Asian Earth Sciences* 42, no. 6 (2011): 1309-1323.

Robb, Laurence. *Introduction to ore-forming processes*. John Wiley & Sons, 2013.

Rohs, C. Renee, and W. R. Van Schmus. "Isotopic connections between basement rocks exposed in the St. Francois Mountains and the Arbuckle Mountains, southern mid-continent, North America." *International Journal of Earth Sciences* 96, no. 4 (2007): 599.

Rohs, Renee C. "Timing of Thermal Overprints in the Silvermines Granite and Associated Diabase Intrusions, St. Francois Mountains, Missouri." *The Compass: Earth Science Journal of Sigma Gamma Epsilon* 85, no. 3 (2013): 2.

Rowe, R. R., and X. Zhou. "Models and exploration methods for major gold deposit types." In *Proceedings of Exploration*, vol. 7, pp. 691-711. 2007.

Shelton, K. L., Lofstom D. M. "Stable isotope and fluid inclusion studies of W-Sn-Ag deposits, Silver Mine district, southeastern Missouri: Tectonic control of water-rock interaction in a magmatic hydrothermal system." In *North American Conference on Tectonic Control of Ore Deposits and the Vertical and Horizontal Extent of Ore Systems.*, pp. 368-377. University of Missouri-Rolla, 1988.

Siddiqui, R. H., Z. Khan, and S. A. Hussain. "Xenothermal alteration and tungsten mineralization in Saindak area, Baluchistan, Pakistan." *Act Min Pak* 2 (1986): 74-77.

Sidorov, A. A. "Xenothermal ore deposits of Northeastern Russia." In *Doklady Earth Sciences*, vol. 433, no. 1, pp. 861-865. MAIK Nauka/Interperiodica, 2010.

Singewald, Joseph Theophilus, and Charles Milton. "Greisen and associated mineralization at Silvermine, Missouri." *Economic Geology* 24, no. 6 (1929): 569-591.

Sugaki, A. "Geological study on the ore deposits in the La Paz district, Bolivia." *Sci. Rept. Tohoku Univ., Ser. III* 16 (1985): 131-198.

Taylor, Stuart Ross, and Scott M. McLennan. "The continental crust: its composition and evolution." (1985).

Tilton, George R., G. W. Wetherill, and G. L. Davis. "Mineral ages from the Wichita and Arbuckle mountains, Oklahoma, and the St. Francis mountains, Missouri." *Journal of Geophysical Research* 67, no. 10 (1962): 4011-4019.

Tolman, Carl. *The Geology of the Silver Mine Area: Madison County, Missouri*. Missouri Bureau of Geology and Mines, 1933.

Tomlin, Katherine. "X-ray Diffraction and Petrographic Analyses of the Large Diabase Dike Intruding the Silvermines Granite in SE Missouri." In *Geological Society of America Abstracts with Programs,* vol. 40, no. 3, p. 8. 2008.

Wahlstrom, Ernest Eugene. "Ore deposits at Camp Albion, Boulder County, Colorado." *Economic Geology* 35, no. 4 (1940): 477-500.

White, Noel C., and Jeffrey W. Hedenquist. "Epithermal gold deposits: styles, characteristics and exploration." *SEG newsletter* 23, no. 1 (1995): 9-13.

Yokoro, Yu, and Kazuo Nakashima. "Ag-Cu-Pb-Bi-S Minerals Newly Discovered from the Ohori Base Metal Deposit, Yamagata Prefecture, NE Japan: Implications for Bi-metallogenesis in the Green-Tuff Region." *Resource geology*60, no. 1 (2010): 1-17.

# VITA

Daniel Joseph Warbritton is from Peoria, IL. He served honorably for four years (2010-2014) in the United State Marine Corps as an infantry machine-gunner. After the Marine Corps, he attended Illinois State University and earned his Bachelor of Science in Geology in May of 2017. He attended graduate school at the Missouri University of Science and Technology, and received his Master of Science in Geology and Geophysics in December of 2019.